Integrating transitional-flow signatures into hybrid event beds: Implications for hybrid flow evolution on a submarine lobe fringe

Łapcik, Piotr; Baas, Jaco

Journal of Sedimentary Research

DOI:
10.2110/jsr.2024.023E

E-pub ahead of print: 04/09/2024

Peer reviewed version

Integrating transitional-flow signatures into hybrid event beds: Implications for hybrid-flow evolution on a submarine lobe fringe

Piotr Łapcik[1] & Jaco H. Baas[2]

[1] *Institute of Geological Sciences, Jagiellonian University, Gronostajowa 3a, PL-30-387 Kraków, Poland*

[2] *School of Ocean Sciences, Bangor University, Menai Bridge, LL59 5AB, Wales, U.K.*

ABSTRACT

Alongside turbidites and debrites, hybrid event beds are now recognized as a common occurrence in deep-marine environments. Yet, many variations in the standard H1–H5 facies model of Haughton et al. (2009, Marine & Petroleum Geology, 26, 1900–1918) have been described since its introduction, with the role of transient-turbulent flows, i.e., flows that are transitional between fully turbulent turbidity currents and fully laminar debris flows, being particularly enigmatic.

Based on a comprehensive dataset collected from the lobe fringe and distal fringe of a submarine fan (Silurian Aberystwyth Grits Group and Borth Mudstone Formation, West Wales, United Kingdom), transitional-flow signatures were integrated into the standard hybrid-event-bed model. These signatures include muddy sandstones and sandy mudstones with large ripples (formed by turbulence-enhanced transitional flows), low-amplitude bed waves and heterolithic lamination (formed by turbulence-attenuated transitional flows), and banding (formed by turbulence-enhanced to turbulence-attenuated transitional flows).

The field data reveal that: (a) H1-divisions are generated by turbulent flows that form not only massive, structureless facies but also plane-parallel-laminated and ripple-cross-laminated facies; (b) H2-

divisions are formed by transitional flows that form banded facies, but also facies with large ripples and low-amplitude bed waves, as well as heterolithic facies; (c) H3-divsions are formed by laminar debris flows of varied rheology; (d) H4-divisions can form from both tractional turbulent and transitional flows; and (e) H5-divisions can be hemipelagic, deposited from the dilute tail of the flow or originate from cohesive freezing of a late-stage muddy debris flow.

Based on embedded Markov-chain analysis, the vertical stacking of facies in the five principal hybrid-event-bed divisions suggests a transformation from turbidity current via transitional flow to debris flow (H1 to H3), followed by a repetition of this transformation in the H4 and H5-divisions, but in overall finer-grained sediment. In addition to this complete extended facies model for hybrid event beds, three incomplete bed types could be defined: turbulent-flow-prone, transitional-flow-prone with a H3-division, and transitional-flow-prone without a H3-division.

The sedimentary successions in the study area reveal a basinward change from predominantly turbidites and turbulent-flow-prone hybrid event beds via a mixture of turbulent-flow and transitional-flow signatures in hybrid events beds to H3-missing hybrid event beds with transitional-flow and muddy-debrite signatures. Hence, sediment gravity flows became increasingly muddy and cohesive from lobe fringe to lobe distal fringe.

INTRODUCTION

Bipartite beds bearing sedimentary characteristics of turbidites capped by debrites and tripartite beds consisting of debrites sandwiched by turbidites are known from depositional systems worldwide (e.g., Talling et al. 2004; Haughton et al. 2003, 2009; Davis et al. 2009; Kane and Pontén 2012; Talling 2013; Grundvåg et al. 2014; Fonnesu et al. 2015, 2016, 2018; Southern et al. 2017; Spychala et al. 2017; Kuswandaru et al. 2018; Pierce et al. 2018; Hansen et al. 2019; Baas et al. 2021; Brooks et al. 2022; Pszonka et al. 2023; Siwek et al. 2023). The most widely used facies model of these hybrid event beds

(Haughton et al. 2009) is composed of five divisions (Fig. 1): lower, structureless and dewatered sandstone (H1); banded sandstone (H2); muddy sandstone or sandy mudstone with sand patches, sand injections, outsized granules, and mud clasts (H3); plane-parallel and ripple-cross-laminated sandstone (H4); and upper pseudonodular or massive mudstone (H5). Idealized occurrences of full H1–H5 hybrid event beds in the sedimentary record have been interpreted to record changes in flow type from turbulent (H1: high-density turbidity current) through transitional (H2: transient-turbulent flow) to laminar flow (H3: debris flow), with turbulent flow in the final stage of deposition (H4 and H5: low-density turbidity current followed by suspension settling). Generally, as with other facies models, the complete sequence of divisions is not always present (cf. Bouma 1962; Stow and Shanmugam 1980; Lowe 1982).

The pervasiveness of hybrid event beds in core and outcrop supports their formation by flow transformation between turbidity current and debris flow, rather than the simultaneous occurrence of separate debris flows and turbidity currents in the same area (Haughton et al. 2003, 2009). Flow transformation starts with flow bulking by an erosive turbidity current, possibly with a debritic head (Baas et al. 2021) that rips up mud clasts from the substrate. These clasts at least partly disintegrate whilst moving to the rear of the flow, resulting in the turbidity current being followed by a clast-rich or muddy debris flow, in which cohesive forces outcompete turbulent forces (Baas and Best 2002; Haughton et al. 2003; Talling et al. 2004; Amy and Talling 2006; Baas et al. 2009, 2011). A muddy erodible substrate thus plays an important role as a source of the cohesive clay, although coarser, non-cohesive sediment can also become incorporated in the debris flow. In addition to longitudinal segregation (Haughton et al. 2003; 2009; Kane and Pontén 2012), vertical segregation and a combination of both (Baas et al. 2011, 2021) have been proposed to explain the formation of hybrid event beds. Moreover, there has been debate on whether a turbidity current or debris flow forms at the front of the hybrid flow (Haughton et al. 2009; Talling 2013; Baas et al. 2021). Since Haughton et al. (2009) proposed their hybrid-event-bed model, complementary models have been proposed, based on facies-tract observations and spatio-temporal changes in vertical and longitudinal structure of the hybrid flow (e.g., Kane and Pontén 2012; Talling 2013; Fonnesu et al. 2015, 2018; Kane et al. 2017; Southern et al. 2017; Pierce et al. 2018; Baas et al. 2021).

Hybrid event beds have been described predominantly from the outer parts and lateral margins of submarine fans, specifically on distal and lateral fringes of depositional lobes and the basin floor beyond lobes (e.g., Talling et al. 2004, 2007; Barker et al. 2008; Davies et al. 2009; Haughton et al. 2009; Hodgson 2009; Grundvåg et al. 2014; Southern et al. 2017; Spychala et al. 2017; Fonnesu et al. 2018), and more rarely from proximal settings, such as the channel–lobe transition zone (Terlaky and Arnott 2014; Pierce et al. 2018; Baas et al. 2021; Mueller et al. 2021). Hybrid event beds have broad application (Haughton et al. 2003): (a) as a tool for predicting depositional setting and sedimentary process, marking changes in the equilibrium profile of the basin and recording the response of depositional systems to tectonic uplift and sea-level change; (b) as indicator of the influence of seafloor topography and basin confinement on flow transformation; and (c) as indicator of spatio-temporal flow evolution, contributing to a better understanding of the full spectrum of flow types between turbulent and laminar flow. Examples of their industrial application include carbon sequestration and hydrocarbon exploration, because of their ability to form low-permeability baffles and barriers to fluid flow in potential reservoir rocks.

Despite extensive past research on hybrid flows, much remains to be explored. Deep-sea sedimentary systems are constructed by sediment gravity flows that involve a variety of sedimentary processes, often co-occurring in a single event (Haughton et al. 2009; Mulder 2011; Pickering and Hiscott 2015; Stow and Smillie 2020). This leads to a wide spectrum of possibilities for hybrid-flow evolution and their expression as hybrid event beds in the sedimentary record (Talling et al. 2004, 2007; Amy and Talling 2006; Kane and Pontén 2012; Patacci et al. 2014; Pierce et al. 2018; Peakall et al. 2020; Baas et al. 2021). Attention has focused on the role of turbidity currents and debris flows, as end members of flow behavior, in the evolution of hybrid flows (e.g., Haughton et al. 2009; Talling 2013; Fonnesu et al. 2016, 2018). However, the precise role of transitional flows, with turbulence-enhanced and turbulence-attenuated behavior (Baas and Best 2002; Baas et al. 2009, 2011), on the transfer and deposition of sediment is still largely unknown (Lowe and Guy 2000; Kane and Pontén 2012; Baker and Baas 2020). Herein, superbly exposed outcrops in the Silurian Aberystwyth Grits Group and Borth Mudstone Formation of west Wales, U.K., were analyzed to help fill this gap in knowledge. Almost 200 hybrid event beds and co-occurring events beds were logged in the lobe-fringe region of the Silurian submarine fan, as defined by Baker and Baas (2020), with the aim to record mm and cm-scale sedimentary features related to laminar (i.e., turbulence-suppressed), transitional (i.e., turbulence-modulated), and turbulent flows. This approach revealed a wide range of bipartite and tripartite hybrid event beds with internal structures that allowed reconstruction of the temporal and spatial evolution of the flows that formed these beds. Based on a comparison with contemporary hybrid-event-bed models, a more comprehensive facies model for hybrid event beds that extends evidence for deposition from transitional flows is proposed.

GEOLOGICAL SETTING

A 6.7-km long transect in the Silurian Aberystwyth Grits Group and Borth Mudstone Formation was studied. This exceptionally well-exposed continuous outcrop in coastal cliffs between Aberystwyth and Borth in west Wales, U.K. (Fig. 2), which was originally part of a deep-marine Cambrian–Silurian back-arc basin, the Welsh Basin, is on the northern limb of an open, east–west striking, synclinal structure. Part of the basin fill is exposed over a distance of c. 40 km between the villages of Cwmtydu in the south and Borth in the north (Fig. 2). The formation of the Aberystwyth Grits Group and Borth Mudstone Formation in the upper Llandovery is associated with the collision of the Avalonia microcontinent with Laurentia, which resulted in major uplift to the south of the study area, and a phase of extensional faulting that provided accommodation space for deposition of deep-marine sediment sourced from the orogeny (Cherns et al. 2006). The Welsh Basin thus formed has been described as a linear upper-crustal fault trough, tectonically constrained by the Bronnant Fault to the east and south-east (Gladstone et al. 2018). The majority of the deposits in the Aberystwyth Grits Group were formed by sediment gravity flows on a submarine fan (Gladstone et al. 2018). In general, the deposits show textural and structural changes from more proximal at Cwmtydu to more distal at Borth (Davies et al. 1997; McClelland et al. 2011; Baker and Baas 2020; Baas et al. 2021). These changes include a basinward decrease in grain size, thinning of event beds and thickening of interbedded mudstones, and increase in mud content (Wood and Smith 1958; Wilson et al. 1992; Smith 2004; Talling et al. 2004; Cherns et al. 2006; McClelland et al. 2011).

Deposits in the southern part of the Aberystwyth Grits Group are mostly represented by medium to thick-bedded, muddy sandstones and Bouma-type turbidite beds (Bouma 1962; Baas et al. 2021). Northwards, in the area between Aberarth and Clarach Bay (Fig. 2), the thick sandstones are replaced by thinner sandstones with a predominance of T_b–T_e and T_c–T_e turbidites and hybrid event beds (Talling et al. 2004; Baker and Baas 2020). Ultimately, near Borth in the north, the Borth Mudstone Formation is dominated by medium to thin-bedded T_c–T_e turbidites, separated by thick-bedded mudstones, formed by hemipelagic deposition and muddy gravity flows (Baker and Baas 2020). Besides downslope fining and thinning of deposits, similar trends occur stratigraphically upward (McClelland et al. 2011). The study area represents a relatively distal sedimentary environment, interpreted as depositional lobe fringe (between Aberystwyth and Harp Rock) and distal fringe (between Harp Rock and Borth) (Fig. 2; Baker and Baas 2020).

METHODOLOGY

The sedimentological research in the study area comprised the collection of detailed, mm and cm-scale, sedimentary logs, with a focus on sedimentary facies that record the depositional process of turbulent, transitional, and laminar-flow types. The area between Aberystwyth and Borth was subdivided into seven smaller areas (I–VII in Fig. 2B), based on changes in dominant type of deposit and characteristic landmarks. The approximate lengths of the areas I to VII were 1.2 km, 0.28 km, 0.31

km, 0.87 km, 0.35 km, 2 km and 1.43 km, respectively. The sedimentary logs document bed lithology, bed thickness, textural properties, primary depositional, erosional and deformational sedimentary structures, and descriptions of lower and upper surfaces, supplemented with digital photographs. The classification scheme of sedimentary facies and facies associations in the study area of Baker and Baas (2020) was adopted in the present study, but with some extensions to include different hybrid-event-bed divisions, described below. The deposits recorded in the different areas were considered the spatial representation of a gradual shift in depositional environment from lobe fringe to distal fringe, in support of Baker and Baas (2020). Embedded Markov-chain analysis was used to establish vertical facies-transition trends separately in the hybrid event beds with division H3 (n = 99) and without division H3 (n = 81) (see Davis 2002 for details). The analysis started by counting each transition between event-bed divisions and the preparation of a transition-count matrix. Next, a transition-probability matrix for the event-bed divisions was calculated by dividing the number of occurrences of a division transition by the sum of all the division transitions for that division. In the next step, an independent trials-probability matrix was prepared by dividing the number of occurrences of a particular division by the number of occurrences of all divisions different from this division. Finally, a difference matrix was created by subtraction of the transition-probability matrix from the independent trial-probability matrix.

RESULTS

Eight sedimentary facies were described in the study area and subsequently categorized in five facies associations, using Markov chain analysis, by Baker and Baas (2020; their figures 2 and 8). Below, these facies and facies associations are briefly described, and expanded by adding a nineth facies (Table 1, with facies codes given in Table 2). Novel data on facies associations 4 (clast-rich hybrid event beds) and 5 (transitional-flow deposits) are described in detail thereafter, based on the present field study. These descriptions focus on transitional-flow signatures in the H1–H5 divisions of hybrid event beds (*sensu* Haughton et al. 2009) and in event beds that do not fit the Haughton et al. (2009) model, vertical facies transitions in the event beds, and longitudinal changes in bed types in the field area.

Sedimentary Facies

Massive sandstone.—The massive-sandstone facies consists of very-fine-grained to medium-grained, structureless sandstone with a light blue–grey color. Most sandstones lack vertical grading, and have sharp, flat bases and sharp tops. Some massive sandstones gradually fine upward or have wavy tops.

The fining-upward massive sand was formed by rapid settling of suspended particles from high-concentration, turbulent or transitional, sandy gravity flows (Arnott and Hand 1989; Kneller 1995; Kneller and Branney 1995; Baas et al. 2009, 2011; Talling et al. 2012), whereas the ungraded massive sand was more likely formed by en-masse cohesive or frictional freezing of sandy debris flows or high-density turbidity currents (Shanmugam and Moiola 1995; Mulder and Alexander 2001; Talling et al. 2012). The wavy tops of the massive-sandstone facies are attributed to post-depositional deformation, potentially involving dewatering after rapid deposition of the sand.

Structured sandstone.—This facies consists of fine to medium-grained, structured sandstone with a low mud content and a light blue–grey color. Depositional structures include plane-parallel lamination, angle-of-repose ripple cross-lamination, and rare wavy lamination and convoluted lamination. The sandstone lacks vertical grading or shows normal grading; structured-sandstone facies with convolute lamination lack grading. Sandstone bases and tops are generally sharp and flat, but occasionally wavy. In some cases, the upper part of the structured sandstone gradually fines upward to mudstone.

The primary current lamination in the structured sandstone facies indicates deposition from turbulent sandy gravity flows, with a lower rate of suspended-sediment settling than for the massive-sandstone facies. A wide spectrum of current velocities allowed formation of upper-stage plane beds and plane-parallel lamination at high velocities and ripple cross-lamination at lower velocities (Allen 1982; Best and Bridge 1992). Waning flow resulted in normally graded deposits, whereas ungraded deposits suggest a more constant flow velocity or settling of well-sorted sand. The wavy lamination observed in the structured-sandstone facies may have formed through soft-sediment deformation of plane-parallel laminae. Some instances of wavy lamination resemble the "sinusoidal ripple lamination" or "draped lamination" described by Jopling and Walker (1968) and Ashley et al. (1982), which was experimentally demonstrated to develop under high rates of suspended-sediment settling onto inactive bedforms (Ashley et al. 1982). The convoluted laminae originated from sediment deformation during or shortly after deposition (Gladstone et al. 2018).

Banded sandstone.—The banded very-fine to fine-grained sandstone facies is characterized by distinctive and closely spaced alternations of dark and light bands. The dark bands may contain small mud clasts and show higher proportions of mud reflected in a dark grey hue of the sandstone. The light bands consist of massive or structured sandstone, including planar-parallel lamination, ripple cross-lamination and wavy lamination. Loading of the light bands into dark bands and other evidence for plastic deformation are frequent. Their thickness ranges from micro to mesobanding (*sensu* Lowe and Guy 2000). The proportion and thickness of the light and dark bands in this facies can be equal, or either can dominate.

The banded-sandstone facies was formed under fully turbulent and tractional flow conditions, recorded in the light bands with structured sandstone (Allen 1982; Best and Bridge 1992), alternating with episodes of flow influenced by turbulence attenuation by cohesive mud, recorded in the dark bands. This facies is considered to represent transitional-flow deposits, reflecting depositional modes pulsating between turbulent and laminar flow (Lowe and Guy 2000; Lowe et al. 2003; Baas et al. 2009; Haughton et al. 2009; Stevenson et al. 2020; Łapcik 2023).

Clast-rich sandstone.—The clast-rich-sandstone facies has a light blue–grey color and comprises very-fine-grained to fine-grained matrix-supported sandstone with scattered clasts of black mudstone and light blue–grey, medium-grained sandstone. This facies is structureless and ungraded, with sharp, flat bases and tops. The size of the clasts ranges from several millimeters to tenths of meters. The clasts are well-rounded and show preferred alignment parallel to the base of the sandstone.

The clast-rich-sandstone facies resembles the deposit of a debris flow or an upper-transitional plug flow, where cohesive clay particles act as support for the sand grains and sand and mud clasts (Iverson 1997; Baas et al. 2009, 2011; Talling et al. 2012). The ungraded and structureless nature of the mud-clast-rich and matrix-supported-sandstone facies indicates en-masse cohesive freezing (Iverson 1997; Mulder and Alexander 2001; Talling et al. 2012). The horizontal alignment of the clasts is further evidence for cohesive turbulence-suppressed flow. However, the flows may have initially exhibited turbulent behavior, resulting in disintegration and rounding of mud and sand clasts after substrate erosion (Fonnesu et al. 2018; Baker and Baas 2020).

Structured muddy sandstone.—The structured-muddy-sandstone facies consists of mixtures of light blue–grey, very-fine-grained to fine-grained sandstone, darker blue–grey mixed sandstone–mudstone, dark blue–grey siltstone, and black mudstone. The sedimentary structures encompass asymmetrical large current ripples (>13 mm in height and >145 mm in length) with angle-of-repose cross-lamination and thin, elongated bedforms with low-angle cross-lamination (at c. 12° angle), i.e., low-amplitude bed waves (Baas et al. 2016; Baker and Baas 2020). The large current ripples are on average 8 mm higher and 133 mm longer than the ripples in the structured-sandstone facies, and they often exhibit supercritical climbing, thus preserving complete ripple profiles (Baker and Baas 2020). Coarsening-upward siltstone and mudstone predominantly underlie the large ripples. Ripple troughs, crests, and stoss sides may include siltstone and mudstone drapes. The low-amplitude bed waves contain varying proportions of sand and mud and occasionally a muddy or silty base. The bases of the structured muddy sandstones are consistently sharp and mostly flat, some displaying undulations, whereas the tops are sharp or fining upward, and flat or wavy.

The structured-muddy-sandstone facies was formed by deposition from rapidly decelerated turbulence-enhanced transitional flow or lower-transitional plug flow, in the case of large ripples, and lower or upper-transitional plug flow, in case of low-amplitude bed waves (Baas et al. 2016; Baker and Baas 2020). The presence of a muddy or silty base as well as mud drapes are evidence for simultaneous bedform migration and suspension fallout of fine sediment (Baas et al. 2016).

Heterolithic sandstone–mudstone.—This facies consists of alternations of fine-grained sandstone and mudstone organized in bands and laminae up to 4 mm thick. The bands show internal plane-parallel and wavy lamination. Upward-thickening mudstone bands and upward-thinning sandstone bands are common. The heterolithic sandstone–mudstone facies may include small bedforms with mud drapes that laterally transition into laminated mudstone. This facies has a higher mud content, thinner bands, and an overall smaller thickness than the banded-sandstone facies. Moreover, it occupies higher positions in the vertical sequence of divisions in event beds, thus forming later in the evolution of deposits than the banded sandstone. The base of the heterolithic sandstone–mudstones is flat and sharp or diffuse, and the top is predominantly flat and sharp.

Several interpretations have been proposed for the formation of heterolithic sandstone–mudstones (Baker and Baas 2020): (i) phases of waxing and waning of mixed sand–mud gravity flows, where sand and mud are deposited at high and low velocity, respectively (Kneller 1995); (ii) alternations of deposition of sand from dilute turbidity currents and suspension settling of hemipelagic mud; (iii) rapidly decelerated and highly depositional transitional sand–mud gravity flows of constant velocity, involving cannibalization of bed material shortly after deposition as a result of reinstated turbulence at decreased flow density (Baas et al. 2016); (iv) a combination of slowly migrating, sandy low-amplitude bed waves (Best and Bridge 1992) and continuous suspension settling of fine sediment (Baas et al. 2016); and (v) slurry flows that experience near-bed shear sorting (Lowe and Guy 2000).

Siltstone.—The siltstone facies comprises dark blue–grey siltstone, either structureless or plane-parallel-laminated. The siltstone facies is normally graded with gradual tops or ungraded with sharp tops. The base of the siltstone facies is sharp and flat and their top is flat.

The siltstone facies is formed by suspension fallout of silt grains from fully turbulent sediment gravity flows or lower-transitional plug flows (Baas et al. 2011), with tractional forces recorded in the plane-parallel lamination (Piper et al. 1984; Talling et al. 2012).

Silty mudstone.—This dark grey, near-black silty mudstone facies has intermediate silt–clay content compared to the siltstone and mudstone facies. The mudstone contains dispersed silt grains in an overall structureless matrix. The lower and upper facies boundaries are sharp.

The silty mudstone is formed by fine-grained sediment gravity flows that are unable to efficiently segregate silt and clay particles, such as upper-transitional plug flows and quasi-laminar plug flows (Baas et al. 2011).

Mudstone.—This facies comprises black, structureless mudstone with some color variation recorded in swirly textures, caused by coherent variations in silt content, directly above silty and sandy facies. The mudstones predominantly have a flat and sharp base and top.

The mudstone facies can be formed by fine-grained components of sediment gravity flows and hemipelagic background sedimentation (Bouma 1962; Talling et al. 2012). The swirly textures are interpreted as the result of en-masse deposition of the plug region of mud-rich, turbulence-attenuated gravity flows (Baas et al. 2011; Stevenson et al. 2014).

Facies Associations

Five facies associations (FA1–FA5) were defined by Baker and Baas (2020), based on Markov chain analysis of vertical facies transitions.

Facies Association 1 (FA1): Fine-grained thin-bedded turbidites and transitional-flow deposits.—Facies association 1 (FA1) consists of isolated, thin-bedded (Tucker 1982) siltstone overlain by mudstone, interpreted as fine-grained turbidites. However, in the distal region near Borth (Fig. 2), the presence of mudstone facies with swirly textures indicates transformation to cohesive flow. Therefore, FA1 may represent the deposits of fully turbulent and transitional, turbulence-attenuated, flows.

Facies Association 2 (FA2): Sandy thin-bedded turbidites.—Facies association 2 (FA2) is composed of massive or structured sandstone with a mudstone or siltstone cap. FA2 also includes heterolithic sandstone–mudstone encased in mudstone. The massive and structured sandstone is formed by turbidity currents. The presence of heterolithic sandstone–mudstone may indicate transient turbulent–laminar flow behavior at a late stage of deposition (Łapcik 2023).

Facies Association 3 (FA3): Medium-bedded turbidites.—Facies association FA3 comprises massive and structured-sandstone, heterolithic-sandstone–mudstone, siltstone, and mudstone facies from base to top. Their vertical order commonly resembles Bouma-type sequences of waning flow (Bouma 1962) or, rarely, waxing flow (Kneller and Buckee 2000). Depending on the presence or absence of massive sandstone, FA3 represents high or low-density-turbidity-current deposits. The heterolithic sandstone–mudstone facies mostly occurs in Bouma T_d-divisions, hence its inferred relation to a waning, fine-grained, cohesive, transitional flow (Baker and Baas 2020).

Facies Association 4 (FA4): Clast-rich hybrid event beds.— Facies association 4 (FA4) is made up of various types of hybrid event bed, which may include full or incomplete H1–H5 sequences. These are the main topic of this paper, described in detail below.

Facies Association 5 (FA5): Transitional-flow deposits.—Facies association 5 (FA5) comprises beds containing structured muddy sandstone, overlain by mudstone, siltstone, structured sandstone, and heterolithic sandstone–mudstone, in order of decreasing probability (Baker and Baas 2020). Some beds contain siltstone or mudstone facies below the structured muddy sandstone facies. Clast-rich sandstone facies is absent from FA5. FA5 is described in further detail below, based on new field observations.

Characteristics of H1–H5 Divisions of Hybrid Event Beds in the Study Area

Division H1: High and low-density-turbidity-current deposits.—The lowermost H1-division of the hybrid event beds (FA4) in the study area consists mainly of fine to medium-grained sandstone and rare coarse-grained sandstone. The sandstone is graded to ungraded, with thicknesses of up to 0.30 m. The H1-division may contain massive sandstone (H1m), 0.02–0.16 m thick, and structured sandstone, 0.01–0.19 m thick, with plane-parallel lamination (H1p), ripple cross-lamination (H1r), wavy lamination, and convolute lamination (Fig. 3). Bouma-type sequences of sedimentary structures are common in the H1-division. H1m and H1p may contain mm to dm-sized mudstone clasts, mostly concentrated near the top or base of the division (Fig. 3D). The base of H1-divisions is sharp, frequently showing a variety of trace fossils and sole marks, including groove marks, skim marks, and spindly and parabolic flute marks. Coarse sand fills some of the flute marks. A few H1-divisions have a highly uneven base with mud injections. The top of H1-divisions is sharp or gradually fining upward because of increasing mud content, and flat to wavy, rippled, or convoluted (Fig. 3). A H1-division is present above the base in 95% of all hybrid event beds, but not necessarily with H1m at its base, as in existing hybrid-event-bed models (e.g., Haughton et al. 2009).

The H1-division is interpreted as the depositional product of a turbidity current, but not limited to a high-density-turbidity-current deposit formed by highly aggradational suspension settling and dampening of bed traction (Lowe 1982; Haughton et al. 2009; Talling et al. 2012). The presence of structured sandstone, in addition to massive sandstone, reveals a more varied origin of the H1-division that includes low-density turbidity currents (cf. Southern et al. 2017), as reflected in the documented Bouma-type sequences. These sequences denote waning high to low-density turbidity currents, if the H1-division starts with massive sandstone, or waning low-density turbidity currents, if the massive sandstone is absent directly above the base. The convolute lamination in the H1-division indicates dewatering and soft-sediment deformation after rapid aggradation and entrapment of pore water. The large variety of sole-mark types supports the complex origin of the H1-division, with, according to

Peakall et al. (2020), fully turbulent turbidity currents forming parabolic flute marks, transitional flows forming spindly flute marks and skim marks, and cohesive, turbulence-suppressed flows forming groove marks. However, some sole marks could have been generated by bypassing flows, unrelated to the formation of the H1-division (Peakall et al. 2020; Baas et al. 2021).

The more complex structure of the H1-division compared to the hybrid-event-bed model of Haughton et al. (2009) matches observations in other hybrid event beds worldwide (Muzzi Magalhanes and Tinterri 2010; Tinterri and Muzzi Magalhanes 2011; Fonnesu et al. 2015, 2018; Southern et al. 2017; Bell et al. 2018). Here, division H1 is interpreted to represent deposition from turbulence-dominated flows, i.e., high and low-density turbidity currents, with a varied evolution of flow types reflected in the stacking of massive and structured-sandstone facies in the division.

Division H2: Transitional-flow deposits.—Division H2 consists of very-fine to fine-grained sandstone with different proportions of siltstone and mudstone. Thicknesses ranges from 0.005 m to 0.155 m, and sedimentary facies include banded sandstone, heterolithic sandstone–mudstone and structured muddy sandstone. The H2-division generally grades upward, with increasing mud content at the expense of sand content. Ideal vertical sequences of facies and sedimentary structures, based on the vertical order of subdivisions in the logged beds, comprise banded facies (H2b) or structured muddy sandstone with large ripples (H2lr) to low-amplitude bed waves (H2bw; Fig. 3E) capped with heterolithic sandstone–mudstone (H2h). However, rarely more than two of these subdivisions were found in one bed. H2h is abundant in troughs of current ripples at the top of H1-divisions and in troughs of large ripples (Fig. 4A); H2h also partially drapes these bedforms. If H2h is present only in the troughs of ripples or large ripples, and these bedforms are immediately below division H3, the vertical sequences of facies change laterally from H1r–H2h–H3 and H2lr–H2h–H3 to H1r–H3 and H2lr–H3, respectively (Fig. 4A). Load structures are frequently developed on the contact surface between the sand-rich and mud-rich deposits, predominantly in divisions H2b and H2h (Figs. 3B, C). Division H2 is present in c. 55% of the hybrid event beds investigated in the field area. In some cases, the H2-division, rather than the H1-division, is present at the base of hybrid event beds (Fig. 4F). Moreover, the banded-sandstone, structured-muddy-sandstone and heterolithic-sandstone–mudstone facies commonly form beds without other divisions typical of hybrid event beds. These beds are described in detail below.

The H2-division contains sedimentary structures typical of transient turbulent flows (*sensu* Baas et al. 2009, 2011, 2016), including banded sandstone (Lowe and Guy 2000; Haughton et al. 2009; Stevenson et al. 2020), large ripples and low-amplitude bed waves (Baker and Baas 2020), and heterolithic sandstone–mudstone (Łapcik 2023). The abundant load structures in this division require a density difference between the muddy and sandy bands (Anketell et al. 1970), and the soft-sediment deformation may have been aided by overpressures generated by abrupt permeability gradients between the muddy and sandy bands. The H2-division presented herein is an extended version of the H2-division of Haughton et al. (2009) that includes the depositional properties of transitional flows observed in the study area.

Division H3: Cohesive laminar-plug-flow deposits.—The H3-division consists of mudstone and sandstone rafts and intraclasts, and sandstone balls and pillows (detached load casts), floating in a muddy-sand to sandy-mud matrix. Thicknesses range from 0.01 m to 0.36 m. The H3-division was described by Baker and Baas (2020) as clast-rich sandstone; five further subfacies are distinguished here: a) muddy sandstone with large rafts (up to 1.05 m long) consisting of mudstone or heterolithic mudstone–siltstone (Fig. 3A); b) poorly mixed muddy sandstone with mudstone clasts and sandstone balls and pillows (Fig. 4D); c) muddy sandstone, lacking mudstone clasts, but with well-preserved sandstone pillows, present at all levels in the H3-division, even near the base (Fig. 3C); d) well-mixed muddy sandstone with small sandstone clasts (pseudonodules), sandstone balls and pillows, and small mudstone clasts (Fig. 3B, D, E); and e) sandy mudstone with streaks of mudstone, siltstone, and sandstone (Fig. 3G), similar to streaky mudstone observed in the H5-division (Baker and Baas 2020). The mudstone clasts appear scattered in the H3-division or concentrated near the top or base of subdivision 1 and 2. Two or three subfacies may be present in a single H3-division, with sharp or gradual boundaries between these subfacies, thus giving the division a bipartite or tripartite appearance (Figs. 3A, F, G, 4E). Bipartite or tripartite H3-divisions predominantly show an upward increase in mud content, with muddier subdivision resting on sandier and less well-mixed subdivisions. Some H3-divisions show faint plane-parallel lamination caused by horizontal alignment of sandstone and mudstone clasts (Fig. 4E).

In accordance with Haughton et al. (2009), the H3-division is interpreted as a debris-flow deposit formed by en-masse cohesive freezing of a laminar plug flow (Iverson 1997; Mulder and Alexander 2001; Talling et al. 2012). The overall chaotic internal structure, with a poorly to well-mixed muddy to sandy matrix and a wide variety of floating clast sizes and distributions, attests to variations in rheology between and within the debris flows (Talling et al. 2012; Talling 2013). These variations are reflected particularly well in the bipartite and tripartite appearance of some H3-divisions (cf. Hussain et al. 2020; Dodd et al. 2022). The most viscous flows are represented by subfacies 1, where large rafts are suspended in the cohesive matrix (Talling et al. 2012). The large rafts may originate from seafloor delamination (Fonnesu et al. 2016). Depending on the rheology, buoyancy may push mud clasts towards the top of the debris flow, but the mud clasts may also concentrate near the base of the flow under their own weight. Mud clasts may experience internal shearing and injection of fine-grained matrix in the debris flow, resulting in clast disintegration reflected in downcurrent downsizing of mud clasts (Fonnesu et al. 2018). Internal shearing may further cause the horizontal alignment of the sand and mud clasts. Debris flows with a relatively poor cohesive-matrix strength allow the sand balls and pillows to occupy all levels in the H3-division. Moreover, the poorly mixed mudstone–sandstone with a variety of clasts of subfacies 2 is interpreted to denote a debris flow with a higher viscosity than the well-mixed muddy sandstone of subfacies 3 and 4. Late-stage loading can be responsible for the sharp boundaries between the load casts and debrite matrix. The balls and pillows may have formed and started to sink into the debris flow while the flow was still moving, especially in shear-thinning quasi-laminar plug flows (Baas et al. 2011; Fig. 4D). The bipartite and tripartite appearance of H3-divisions has been associated with longitudinal segregation and transformation of laminar-flow components (Haughton et al. 2009; Dodd et al. 2022).

Division H4: Low-density-turbidity-current and transitional-flow deposits.—The H4-division of the hybrid event beds (FA4) is up to 0.09 m thick and consists of predominantly normally graded fine-grained sandstone and siltstone. The sedimentary facies include structured sandstone and muddy sandstone with plane-parallel lamination (H4p), ripple cross-lamination (H4r) and low-amplitude bed waves (H4bw), and heterolithic sandstone–mudstone (H4h), which may be deformed as a result of fluid escape and loading into the underlying division (Fig. 3). The base of the H4-division is sharp and flat to strongly uneven and poorly defined because of the loading. At the top, the division gradually fines upwards into the mudstone facies of division H5. The H4-division is present in c. 45% of the hybrid event beds investigated in the field area.

The H4-division is formed by low-density turbidity currents and transitional flows, based on the presence of sedimentary structures associated with turbulent and turbulence-modulated flows, respectively, as in the H1 and H2-divisions described above. Different H4-divisions record turbulent flow only (H4p and H4r), a gradual change from turbulent to transient turbulent–laminar flow (H4p, H4r, H4bw and H4h), and transitional flow only (H4bw and H4h). These flows could constitute the tail of the main core of the hybrid flow or form by mixing of ambient water with sediment from the upper part of the laminar debris flow of the H3-division. The H4-division presented herein is an extended version of the H4-division of Haughton et al. (2009) that was limited to low-density-turbidity-current deposits. We argue that division H4 may also include transitional-flow deposits, which agrees with the flow-evolution model for lobe distal fringes of Baker and Baas (2020).

Division H5: Hemipelagic and transitional-flow deposits.—Division H5 comprises silty-mudstone and mudstone facies at the top of each hybrid event bed in the field area. Thicknesses range from c. 0.04 to 0.38 m, and some of the mudstones show swirly or pseudonodular textures (Haughton et al. 2009; Baker and Baas 2020).

The H5-division may be formed by slow settling of hemipelagic sediment, gradual suspension settling of mud from the dilute tail of the hybrid flow (Haughton et al. 2009; Pierce et al. 2018), updip remobilization of the top of the H3-division (Obradors-Latre et al. 2023) and rapid deposition from waning fine-grained cohesive flows (Baas et al. 2011). Baker and Baas (2020) showed that part of thick mud caps in the lobe distal fringe of the deep-marine system near Borth (Fig. 2) were deposited en-masse from upper-transitional and quasi-laminar plug flows that bypassed more proximal areas or transformed from muddy suspensions up-dip.

Deposits Other than Hybrid Event Beds and Bouma-Type Turbidites

In the study area, transitional-flow deposits were previously recognized by Baker and Baas (2020) from the presence of large ripples and low-amplitude bed waves. The present field study found a greater variety of transitional-flow deposits, with sedimentological properties that are similar to the H1, H2, H4 and H5-divisions of the hybrid event beds. However, the transitional-flow deposits differ from the hybrid event beds in the lack of a H3-division, i.e., a debris-flow signature.

If present, the H1-division of the transitional-flow deposits contains classic Bouma-type H1m, H1p and H1r facies (Fig. 5B, C, D, F). Division H2 bears sedimentary structures indicative of transitional flow, including H2b, H2lr, H2bw and H2h-facies. Rather than being capped by a H3-division, the H2-division of transitional-flow deposits is overlain by H4p and H4r-facies, formed by turbulent flows, H4bw and H4h-facies, formed by transitional flows, or directly by H5-mudstone facies (Fig. 5). The distinction between divisions H2 and H4 is straightforward if turbulent-flow facies separate transitional-flow facies, in which case the vertical sequence is limited to H2-transitional-flow facies – H4-turbulent-flow facies – H4-transitional-flow facies (Fig. 5D). However, in the absence of turbulent-flow facies, some features can be used to distinguish the H2 and H4-transitional-flow facies: 1) abrupt grain-size change from medium and fine-grained sand to very-fine-grained sand and silt without a change in sedimentary structure (Fig. 5F); 2) decrease in sand-to-mud ratio, increase in muddiness, and presence of mud drapes and streaks (Fig. 5A); and 3) reduction in the wavelength and height of bedforms (Fig. 5F). Moreover, matching with the facies characteristics of the hybrid event beds described above, large ripples are limited to the H2-division.

Markov-Chain Analysis of Vertical Transitions

Hybrid event beds.—Embedded Markov-chain analysis was conducted to statistically capture the large variety of hybrid event beds (n = 99) and transitional-flow deposits (n = 81) in the study area (Figs. 3–5). Figure 6 shows separate difference matrices for hybrid event beds (Fig. 6A) and transitional-flow deposits (Fig. 6B), plotted onto the original hybrid-event-bed model of Haughton et al. (2009). These matrices were used as a proxy for flow evolution by determining the most common single and multi-level vertical transitions of sedimentary facies. Most hybrid event beds have a lowermost H1-division with a wide variety of facies transitions (Fig. 6A). H1m above the base of the H1-division mostly changes upward to H1p or H1r, reflecting a reduction in sediment-fallout rate and a shift to tractional transport in turbulent flow. The embedded Markov-chain analysis reveals that transitions from H1m to the banded division H2 in the study area are rare, and therefore show low statistical significance. This differs from the hybrid-event-bed model of Haughton et al. (2009), in which H1m to H2 is the only transition. Here, H1p and H1r commonly appear between H1m and H2, thus denoting a waning turbidity current before the H2-division is formed. Most common is an upward change from H1p to H1r, denoting a waning low-density turbidity current. Transitions from H1p to H2lr or H2b, denoting a temporal change to turbulence-enhanced transitional flow or lower-transitional plug flow, have the lowest probability. H1r shows a strong tendency to change upward to different H2-facies, i.e., H2b, H2bw and H2h, reflecting a gradual transformation from low-density turbidity current to turbulence-modulated transitional flow. Direct transitions from H1r to H3 are the least probable, whereas direct transitions from H1p to H3 have a significantly higher probability. In summary, the Markov-chain analysis confirms the visual observations described above that division H1 was formed by classic, Bouma-type, turbidity currents of low and high density (Bouma 1962; Lowe 1982; Southern et al. 2017) that transform into transitional flows or directly into laminar debris flow.

In Figure 6A, H2b represents the lowermost part of the H2-division. H2b is equivalent to plane-parallel lamination under transitional plug flow (Stevenson et al. 2020) or signifies the migration of low-amplitude bed waves, as in the experiments of Baas et al. (2016). The most common transitions in division H2 are from H2b, H2lr or H2bw directly to H2h. Vertical sequences that comprise three or four facies in division H2 are less likely, shown by the absence of H2b–H2lr transitions, and the low probabilities of H2b–H2bw and H2lr–H2bw transitions (Fig. 6A). The most probable transitions to division H3 are from H2bw and H2h. H2h fills the trough of ripples and low-amplitudes bed waves and drapes these bedforms before the debris flow arrives; H2h may thus signify near-laminar, upper-transitional plug flow. Overall, division H2 shows a trend of transformation to progressively more cohesive flow as a result of increased mud concentrations and flow deceleration, which may have started in division H1 with the vertical sequence H1m–H1p–H1r.

More than half of the clast-rich sandstone of the H3-division is capped by the mudstone of division H5 (Fig. 6A). If there is an intercalated H4-division, the clast-rich sandstone transitions to structured sandstone of H4p or H4r, indicating a change from debris flow to low-density turbidity current, or to structured muddy sandstone of H4bw and H4h, signifying a change from debris flow to transitional flow (Fig. 6A). As mentioned above, these changes in flow type may denote the tail of the hybrid flow or mixing of ambient water with sediment from the upper part of the laminar debris flow of division H3.

In division H4, H4p transitions rarely to H4r, and vertical changes from H4p to H4bw/h are statistically insignificant (Fig. 6A). In contrast, the probability of H4bw/h overlying H4r is high. This suggests that waning low-density turbidity currents are less common than transitional flows and low-velocity, low-density turbidity currents transforming to transitional flows in this part of the basin. This transformation can be achieved by incorporation of sediment from division H3 below followed by flow waning, thus promoting cohesion, or by supply of excess mud from the upstream tail of the flow. Figure 6A shows a high probability that H4p, H4r and H4bw/h are overlain by H5, which may either represents hemipelagic deposition, dilute tail of hybrid flow or muddy-debris-flow freezing. It is most likely that the transition from H4p or H4r to H5 involves the progression from low-density-turbidity-current deposition to hemipelagic deposition, and the change from H4bw/h to H5 (possibly underlain by H4r) comprises the progression from transitional-flow deposition to muddy-debris-flow freezing (with a possible precursor of turbidity-current deposition).

Transitional-flow deposits.—Figure 6B summarizes the embedded Markov-chain analysis for the transitional-flow deposits, which lack a H3-division. The transitions between subdivisions within and between the H1 and H2-divisions in the transitional-flow deposits are similar to those in the hybrid event beds, but there are notable differences in some of the transition probabilities. In the transitional-flow deposits, transitions from H1m to H2b and H2lr are more common than transitions from H1m to H1p and H1r. This suggests that flow transformation from turbidity current to turbulence-modulated transitional flow commonly lacks a tractional phase. This contrasts with the hybrid event beds, in which the sequence H1m–H1p–H1r–H2 is most common (Fig. 6A). Moreover, the probability of transitioning from H1p to H2lr is higher than in the hybrid event beds, and H1r is overlain exclusively by H2bw, rather than by four different H2-subdivisions in the hybrid event beds (Fig. 6). These results imply a more abrupt turbulent to transitional-flow evolution, hence more rapid turbulence modulation, than in the hybrid events. Alternatively, the high probability of H1m–H2 transitions in the transitional-flow deposits may indicate that H1m resulted from rapid deposition of sand from a high-density transitional flow with limited turbulent support and some cohesive support (Baas et al. 2011; their figure 20).

H2b and H2lr are common in the transitional-flow deposits, as expected, but H2bw is relatively rare. This scarcity may be linked to the missing laminar-flow division H3, since low-amplitude bed waves form in strongly turbulence-attenuated transitional flows (Baas et al. 2011). In contrast, H4bw is common in both hybrid event beds and transitional-flow deposits. In division H2, the highest variability of facies transitions is recorded in H2b (Fig. 6B). It shows similar probability of transition to H2h, H4p, H4r, and H4bw/h. However, in contrast with the hybrid event beds, the highest transition probability is directly to H5 instead of to H2h.

As in the hybrid event beds, H2lr most frequently passes into H2h. For the other H2-subdivisions, a direct transition to H5 has the highest probability (Fig. 6B), which renders paths of flow evolution simpler than for the hybrid event beds. Three main paths can be distinguished: (1) H2b–H2h–H5 or H2lr–H2h–H5, signifying a gradual change to weaker and muddier transitional flow, ending in laminar mud flow or hemipelagic deposition; (2) H2b–H4p–H5 or H2b–H4r–H4bw/h–H5, indicating an increase in turbulence in the late stages of the flow — in the turbulent tail of the flow or due to admixture of ambient fluid on top of the transitional flow or a bypassing debris flow — and possibly followed by a final return to strongly cohesive and turbulence-attenuated or laminar flow upon flow deceleration; and (3) direct transition from the H2-subdivisions to the H5-division, which most likely represents a change from transitional flow to quasi-laminar flow and deposition of fluid mud.

The transition probabilities within division H4 and from division H4 to H5 in the transitional-flow deposits are similar to those in the hybrid event beds, except for a statistically insignificant transition from H4r to H5 in the transitional-flow deposits (Fig. 6). This transition is replaced by a more common H4r–H4bw/h transition, which signifies a slight shift away from the evolution of turbulent flow to hemipelagic deposition towards the evolution from turbulent to transitional, and possibly laminar, flow in divisions H4 and H5.

Integrated hybrid event beds and transitional-flow deposits.—Informed by the key finding that the hybrid event beds and transitional-flow deposits share common sedimentological features, have the same subdivisions, and their flow-evolution trees complement each other to a large degree (Fig. 6), separate embedded Markov-chain analysis was conducted by integrating the datasets for both these facies associations (Fig. 6C). This analysis aimed to find support for the hypothesis that the transitional flows are a subset of a wider spectrum of hybrid flows that include quasi-laminar and laminar-flow regimes.

Figure 6C shows that divisions H1, H2, H4 and H5 preserve most of the evolution of deposition from the transitional flows and hybrid events, with transition probabilities similar to or intermediate between those shown in Fig. 6A and B. Notable deviations are a shift from H1p–H2lr to H1p–H3 in transition probability, as well as a lack of statistically significant H2b–H3, H2b–H4p and H2bw–H3 transitions, in the integrated dataset. These deviations suggest that H2-divisions are more common in transitional-flow deposits than in hybrid event beds and they match the absence of the banded H2-division in many hybrid event beds of the Haughton et al. (2009) type elsewhere (Tinterri and Muzzi Magalhaes 2011; Patacci et al. 2014; Southern et al. 2017; Fonnesu et al. 2018; Pierce et al. 2018; Stevenson et al. 2020; Baas et al. 2021). The integrated flow-evolution tree of Fig. 6C agrees with the trees for transitional-flow deposits and hybrid event beds in H2h being the most important subdivision in H2; H2h thus provides a central link between turbulent flow (H1), transitional flow (H2 and H4), and laminar flow (H3 and H5). In H4 and H5, the integrated flow-evolution tree (Fig. 6C) more closely matches the evolution tree of hybrid events (Fig. 6A) than that of transitional flows (Fig. 6B). This is inevitable, because the integrated-flow and hybrid-event-evolution tree both have a H3-division, but the close link between all three trees after removal of transitions to and from H3, together with the overall small number of deviations, described above, provides strong evidence that the transitional-flow-evolution tree shown in Fig. 6B is a subset of the flow evolution trees shown in Fig. 6A, C.

Terminology Update and New Hybrid-Event-Bed Model

The field data presented herein, along with the statistically significant results (based on χ^2 tests) of the embedded Markov-chain analysis, reveal a close relationship between hybrid event beds and transitional-flow deposits. This leads us to propose a new terminology for hybrid event beds. From this point onward, the term 'hybrid event bed' refers to beds with any mixture of turbulent, transitional and laminar-flow H-divisions. Hence, all three bed types in Fig. 6, with or without a H3-division, are considered to be hybrid event beds. Based on the frequency of occurrence in the study area, 'hybrid event beds' can take three different forms: turbulent-flow-prone beds (Fig. 7B), transitional-flow-prone beds with a H3-division (Fig. 7C), and transitional-flow-prone beds without a H3-division (Fig. 7D). Moreover, 'turbulent-flow deposits', 'transitional-flow deposits' and 'laminar-flow deposits' refer to divisions and subdivisions, i.e., facies, in hybrid event beds with turbulent, transitional, and laminar-flow signatures, respectively. Figure 7 also shows a full facies model (Fig 7A) that summarizes all subdivisions in hybrid event beds in the statistically significant vertical order (based on Chi^2 test) specified by the embedded Markov-chain analysis and original Haughton *et al.* (2009) hybrid-event-bed model. The proposed extended hybrid-event-bed model is described and interpreted in the Discussion section below.

Longitudinal Changes in Hybrid-Event-Bed Properties Between Aberystwyth and Borth

The most proximal part of the study area, north of Aberystwyth (Area I; Fig. 2) is dominated by Bouma-type turbidites (Bouma 1962) and fewer, relatively thin, transitional-flow deposits (Fig. 8) with structured-muddy-sandstone and heterolithic-sandstone–mudstone facies that exhibit upward increasing mud content (Table 3; Fig. 9A). The lowermost division of most hybrid event beds with division H3 in Area I consists of H1p or H1r, whereas similar amounts of transitional-flow-prone hybrid event beds without division H3 commence with H1–H2 or H2-subdivision sequences (Table 3). The vast majority of the hybrid event beds lack a H3-division, but, if present, the sand and mud in the H3-division are well mixed, exhibiting swirly textures. Convolute lamination is abundant in Area I. Almost all hybrid event beds in Area I have a H2-division and 70% of H4-divisions contain only H4p and H4r (Table 3). Flute marks are the most common type of sole mark in Area I (Table 3).

The proportion of hybrid event beds with a central H3-division increases from Area I to Areas II and III, both near Clarach Bay, at the expense of transitional-flow-prone hybrid event beds without a H3-

division (Fig. 9A). In Area III, the hybrid event beds reach a mean thickness of 0.37 m, compared to 0.19 m in Area II and 0.14 m in Area I (Fig. 8A), with H3-divisions contributing most to the bed thickness (Fig. 8B). This rapid downflow increase in bed thickness is caused mainly by thickening of H3 and H5-divisions, but division H4 is also relatively thin in Area I (Fig. 8). Lowermost H1-divisions with Bouma-type sequences (Fig. 9B, C) were observed in most hybrid event beds, whereas H2-divisions are less common than in Area I (Table 3). Despite the overall dominance of hybrid event beds with a H1-divison, equal numbers of transitional-flow-prone beds without a H3-division start with H1 and H2-divisions. H4-divisions, predominantly with plane-parallel lamination and ripple-cross lamination, are common in hybrid event beds with a H3-division, but almost absent in beds without a H3-division. As in Area I, flute marks outnumber groove marks and discontinuous tool marks (skim and prod marks) in Area III. In contrast, the hybrid event bed in Area II have more tool marks than flute marks (Table 3).

Area IV, halfway between Clarach Bay and Wallog (Fig. 2), is characterized by a mixture of hybrid-event-bed types, with transitional-flow-prone beds without a H3-division outnumbering beds with a H3-division (Table 3; Fig. 9A). Average hybrid-event-bed thickness is higher than in Area I, but lower than in Area III, caused by a large decrease in thickness of H3 and H5-divisions and a smaller decrease in the thickness of most other divisions (Fig. 8). The mixed nature of bed properties is further reflected in that: (a) Bouma-type sequences are common in division H1; (b) the lowermost division of transitional-flow-prone beds without a H3-division can consist of H1 or H2 (Fig. 9B); (c) approximately half of the beds with division H3 also contain division H2; (d) the vast majority of H4-divisions have H4bw and H4h; and (e) the number of flute marks and tool marks are evenly spread (Table 3). In Area IV, bipartite and tripartite subdivisions begin to make up a significant proportion of H3-divisions, which was also observed in Areas VI and VII.

Area V and VI, between the cliffs south of Wallog and Harp Rock (Fig. 2), have the highest proportions of hybrid event beds with a H3-division (Fig. 9A; Table 3). At these locations, most hybrid event beds show a full spectrum of H1–H5 divisions, and their mean thickness is somewhat larger than in Area IV, with relatively thick H1-divisions in Area V (Fig. 8). Lowermost H1-divisions that form Bouma-type sequences dominate; fewer hybrid event beds commence with H2lr (Fig. 9B, C). Despite the dominance of full H1–H5-sequences, H4-divisions were not observed in the hybrid event beds of Area V. In Area VI, 30% of H4-divisions contain only H4p and H4r; the remaining H4-divisions have H4bw/h (Table 3). H3-divisions often consist of well-mixed sand and mud with swirly textures (Area VI) or small mud clasts and pseudonodules (Area V). Area V differs from Area VI in that the base of hybrid event beds in Area V is dominated by skim, prod and groove marks, whilst in Area VI flute marks are more common than tool marks (Table 3).

The proportion of hybrid event beds with a H3-division in the most distal Area VII, near Borth, is much lower than in Areas V and VI (Fig. 9A); this was also recognized by Baker and Baas (2020). Instead, H3-missing transitional-flow-prone hybrid event beds composed of structured muddy sandstone with large current ripples and low-amplitude bed waves capped by mudstone with swirly textures (cf. Baker and Baas 2020) are abundant (Fig. 9B, C). These beds consist of H2–H4–H5 and H4–H5-sequences (Fig. 9), with all beds exhibiting H4bw/h and only 38% of beds exhibiting H2-subdivisions (Table 3). Only one hybrid event bed starts with a H1-division, i.e., H1m (Fig. 9B; Table 3). The mean thickness of hybrid event beds and their H-divisions is small and comparable to those in Area I, except for a relatively thick H5-division (Fig. 8). Sole marks are rare in Area VII, but mostly comprise skim marks and groove marks (Table 3).

The size of mud clasts was measured in H1–H3 divisions in Areas I–VI, subdivided into four size classes: <40 mm, 40–99 mm, 100–200 mm, and >200 mm (Fig. 9D). The proportion of the smallest mud clasts generally increases downcurrent at the expense of larger clasts, as previously determined by Baker and Baas (2020). All mud clasts with a size >40 mm are significantly more common in Areas I–IV than in Areas V–VII. Together with an abrupt increase in the proportion of mud clasts <40 mm between Area IV–V, this suggests a sudden disintegration of mud clasts between these areas, possibly at the transition from the proximal to distal lobe fringe. Area VII in the most distal part of the lobe fringe lacks macroscopic mud clasts altogether; presumably all mud clasts were disintegrated between Areas VI and VII.

DISCUSSION

Extended Hybrid-Event-Bed Model — Rationale

The hybrid-event-bed model of Haughton et al. (2009) describes beds that contain evidence for deposition from turbidity currents and debris flows, but it does not include the role of transient-turbulent flows (*sensu* Baas and Best 2002). More recent research on turbulence-modulated flows (e.g., Baas et al. 2009, 2011, 2016; Stevenson et al. 2020; Łapcik 2023) revealed that the spectrum of deposits formed by hybrid events can be much larger, thus justifying the need for expanding the Haughton et al. (2009) model by incorporating more complex depositional processes that leave a record in hybrid event beds. The new field data show that transitional flows can be common in deep-marine environments and they are an integral part of the wide spectrum of sediment gravity flows between turbulent and laminar end members. On the basis of the field data and statistical analysis presented in this study, a more universal facies model that integrates this wider suite of hybrid flows is introduced (Fig. 7). This extended model presents the original hybrid-event-bed model of Haughton et al. (2009) as an end member. Our data suggest that the flow evolution stored in hybrid event beds is more gradual than in the Haughton et al. (2009) model, encompassing a complete, ideal, vertical sequence of turbulent–transitional–laminar–turbulent–transitional–laminar flow–hemipelagic settling (full facies model in Fig. 7), as well as allowing for the formation of incomplete sequences resulting from different flow-evolution paths. Thus, the model distinguishes turbulent-flow-prone hybrid event beds and transitional-flow-prone hybrid event beds with and without evidence for fully laminar-flow conditions in the form of H3- and H5-type debris flows (Fig. 7; Pierce et al. 2018; Hussain et al. 2020), informed by the embedded Markov-chain analysis (Fig. 6). It should be emphasized that, as with any facies model, the extended hybrid-event-bed model is based on a reductionistic approach, and significant deviations from the model are possible, depending on autogenic and allogenic forcings on flow behavior and depositional processes.

Extended Hybrid-Event-Bed Model — Description

In the Haughton et al. (2009) model, the hybrid event beds start with division H1, composed of graded to ungraded, dewatered sandstone, with mud clasts in the upper part of the division. In case of high concentrations of these mud clasts, Fonnesu et al. (2015) defined an additional H1-subdivision (their H1b). These properties are characteristic of rapid sedimentation from non-cohesive high-density turbidity currents. However, more recent literature data (e.g., Muzzi Magalhanes and Tinterri 2010; Tinterri and Muzzi Magalhanes 2011; Fonnesu et al. 2015, 2018; Southern et al. 2017; Bell et al. 2018), as well as data from the study area (Figs. 3–5), indicate a more complex internal character of division H1 (Fig. 7), with sedimentary structures typical of less rapid deposition, including plane-parallel lamination (H1p) and ripple cross-lamination (H1r). These tractional structures may occur above massive sandstone (H1m) or replace it. The formation of division H1 may therefore involve a wide range of low-density to high-density turbidity currents (Talling et al. 2012), thus reflecting the classical turbidite models of Bouma (1962) and Lowe (1982), formed by turbulence-dominated flows (Fig. 7). However, massive sandstone, here H1m, has also been associated with turbulence-attenuated and non-turbulent, cohesive or non-cohesive flows (e.g., Kneller and Branney 1995; Ilstad et al. 2004; Breien et al. 2010; Baas et al. 2011; Hussain et al. 2020).

The facies model depicted in Fig. 7 expands division H2 from banded sandstone (H2b) only (Haughton et al. 2009) to a wider range of facies that indicate deposition from transitional flow (Fig. 7). These facies include large current ripples (H2lr), low-amplitude bed waves (H2bw) (Baas et al. 2016; Baker and Baas 2020) and sandstone–mudstone heterolithics (H2h) (Łapcik 2023), where the large current ripples in the study area are unique to division H2. The wide range of sedimentary structures typical of turbulence-modulated flow in division H2 allows for a more detailed interpretation of the depositional processes and a more precise determination of flow evolution (e.g., Baas et al. 2011, 2016; Baker and Baas 2020; Stevenson et al. 2020), i.e., from turbulence-dominated (H1) via transitional-flow dominated (H2) to laminar-flow dominated (H3) in the full sequence (Fig. 7). Given that the clay content usually increases from H1 to H3, the gradual change from turbulent via transitional to laminar flow is interpreted to be dominated by a gradual temporal increase in the cohesive clay content in these flows. The new facies model reveals the complex nature of division H2, where the vertical stacking of its subdivisions can vary depending on the initial flow conditions and show more diverse evolutionary paths than division H1. However, these variations remain predictable and are limited to the omission of certain subdivisions, rather than random transitions between these subdivisions (Fig. 6).

Hussain et al. (2020) divided division H3 into a relatively sandy lower subdivision, H3a, and a muddier upper subdivision, H3b. In H3a, sand injections and water-escape structures evidence the interaction of the debris flow with previously deposited sand of division H1. H3b represents a more cohesive part of the debris flow that does not interact with the substrate. Dodd et al. (2022) distinguished three subdivisions, H3a–H3c, interpreted as the product of separate flow components formed through rearward longitudinal-flow transformation from weaker cohesive, quasi-laminar plug flow to stronger cohesive, fully laminar plug flow. Differences in flow cohesion were also recognized in the study area based on the five H3-subdivisions (Fig. 7), which show different mud content, size of clasts and degree of internal mixing. However, these subdivisions cannot easily be compared with the facies models of Hussain et al. (2020) and Dodd et al. (2022), because the assumption that “more sand equals less cohesive flow and more clay equals more cohesive flow“ is oversimplified, as sand can make flows more cohesive, especially for high-density turbidity currents and debris flows (Baker and Baas 2023). Moreover, the fact that division H4 can load into the top of division H3, as observed in the study area, means that the upper part of H3 need not represent deposits of highly cohesive flows. Instead, the presence of the load structures suggests that the underlying H3-subdivision can be formed by a weakly cohesive laminar flow with rheological properties resembling a fluid mud. This suggests that the spatio-temporal behavior of the debris flows in the studied part of the Welsh Basin was more complex than in the models of Hussain et al. (2020) and Dodd et al. (2022), with evidence in the stacked H3-subdivisions for increasing or decreasing cohesive-matrix strength of the debris flow. The field data confirm previous observations of decreasing mud clast size in a downflow direction in division H3 (cf. Fonnesu et al. 2018). The widespread occurrence of a wavy top of divisions H1 and H2 on the fringe and distal fringe of lobes in the study area is associated with the preservation of original current-ripple surfaces (cf. Fonnesu et al. 2015), thus suggesting a negligible erosional potential of the debris flows that form division H3. On the other hand, the common convolutions and load structures in divisions H1 and H2 are likely associated with a rapid increase in pore pressure by the sudden emplacement of the debris of division H3 on the previously deposited H1 and H2-divisions.

Division H4 is expanded to incorporate sedimentary structures that evidence turbulence-modulated flow, i.e., low-amplitude bed waves (H4bw) and sandstone–mudstone heterolithics (H4h), above sedimentary structures formed by turbulent flow. i.e., plane-parallel lamination (H4p) and ripple cross-lamination (H4r) (Fig. 7). The extended facies model thus covers different late-stage evolutionary paths of the hybrid flow, where the flow may be represented not only by a low-density turbidity current (Haughton et al. 2009), but also by transitional flows that becomes increasingly cohesive with time, i.e. from lower to upper-transitional plug flow. Baker and Baas (2020) attributed this increase in cohesion to decreasing flow velocity, rather than increasing clay concentration, as in the H1–H3-sequence. The increase in cohesion continues into the H5-division, following the evidence for deposition of silt and clay from quasi-laminar plug flow. However, this does not exclude the formation of division H5 by the dilute tail of the hybrid flow or by hemipelagic sedimentation, especially if H4bw and H4h are absent below the H5-division. An additional mechanism for the formation of increasingly cohesive transitional flow at the late stage of hybrid flow may be the inclusion of mud through interfacial shear between the laminar debris flow (or H3 deposit) and the overriding flow. This mixing process could also have led to weakening of the cohesive forces in the upper part of division H3, thus promoting partial or full loading of H4 sand into H3 mud.

Determining the mode of deposition of mudstones in deep-marine environments based on macroscopic properties has been a major challenge. Understanding the relationship between the sediment below the mudstones and the mudstones themselves, as in this study, can be the key to understanding their depositional conditions. Previous studies have suggested that thick mudstone covers in the distal part of the basin (Borth Mudstone Fm) do not originate from hemipelagic sedimentation (Baker and Baas 2020; Wang et al. 2024, in review). The present study extends this by linking the deposition of mudstone to turbulent low-density turbidity currents in the case of underlying subdivision H4p and H4r, and to transitional flow or quasi-laminar flow in the case of underlying subdivision H4bw/h.

Commented [PŁ1]: Add here or even better in L870: Second flow transformation have been reported in the Ross Fm, where Obradors-Latre et al. (2023) linked the formation of „thin sand-speckled siltstone dvision” in distal setting with up dip remobilisation of the upper part of division H3 with weaker mechanical properties in form of a thinner and more mobile mud flow that. However, this mechanism is excluded for formation of silty divsion H5 underlain by division H4.

See p. 40 in the Obradors-Latre et al., 2023

Or
Prehaps add here cf. Obradors-Latre et al., 2023?

The new hybrid-event-bed model presented here extends the range of textural and structural properties of hybrid event beds, which translates into a better understanding of the spatio-temporal evolution of mixed sand–clay sediment gravity flows and their preservation in the sedimentary record. Despite the increased number of facies types, the vertical order of subdivisions in the facies model remains predictable and informed by gradually changing flow conditions. The turbulence-modulated conditions preserved in divisions H2 and H4 often record gradual flow transformation in the study area, thus serving as a bridge between turbulent and laminar conditions, which is likely applicable also to other sedimentary basins. However, incomplete sequences are numerous, reflected not only in turbulent-flow-prone and transitional-flow-prone beds with and without evidence for laminar flow (Fig. 7), but also in more complex beds that are a reflection of the complex history of flow events. This complex history may involve, amongst others, variations in cohesive clay and non-cohesive sand content, variations in rates of sediment deposition and erosion, flow deceleration and acceleration, and turbulent modulation. Absolute values of flow velocity and suspended-sediment concentration and relative percentages of suspended clay and sand are key controls on degree of turbulence modulation (e.g., Baker et al. 2017; Baker and Baas 2023), and high rates of change of sediment concentration and flow velocity are expected to hinder the preservation of certain flow types in the hybrid event beds (e.g., de Vet et al. 2023). In other words, hybrid events need not comprise all three basic flow types, i.e., turbulent, transitional and laminar, on their way into sedimentary basins or, if they do, signatures of these flow types may not be preserved as a division or subdivision in the final deposit. Examples are: (a) the lack of a H3-division in hybrid event beds because turbulent and transitional-flow behavior dominated at the depositional site, as dispersed clay concentrations were too low to induce laminar flow; (b) the direct transition from H1m to H3, as in the Haughton et al. (2009) model, because rates of deposition were too high to induce transitional flow and the transformation from high-density turbidity current to debris flow was too short to preserve transitional-flow structures; and (c) the lack of a distinct H4-division, because of co-depositional or post-depositional loading into the underlying H3-division.

Longitudinal Trends in Hybrid Event Beds

The overall basinward transition from dominantly turbidites near Cwmtydu and New Quay to dominantly hybrid event beds between Clarach Bay and Borth (Fig. 2) is supported by the field data from Areas I to VII over a distance of 6.7 km. This gradual change in flow type from turbulent to transitional and laminar is recorded in the bed properties, which includes a decrease in the amount of turbidites and a simultaneous increase in the amount of hybrid event beds with transitional-flow signatures in divisions H2 and H4 and laminar-flow signatures in divisions H3 and H5 (Fig.9).

Figure 9 and Table 3 show that there are no simple longitudinal trends in the relative percentages of hybrid-event-bed type. Turbulent-flow-prone hybrid event beds are most common in Area III, transitional-flow-prone hybrid event beds with a H3-division dominate Areas V and VI, and transitional-flow-prone hybrid event beds without a H3-division are present mainly in Areas I, II, IV and VII (Fig. 9).

This may not be surprising, given the many autogenic and allogenic forcings on flow behavior, such as initial flow mobility, flow density and suspended sand–clay ratio, and changes in these parameters between Areas I and VII as a function of changes in slope gradient, bed erodibility, and contrasting rates of deposition of sand and clay. Nonetheless, the sedimentological data collated in Table 3 reveal trends in the relative contributions of turbidity currents, transitional flows and debris flows to the sedimentary successions between Areas I and VII.

Areas I, II and III are dominated by turbulent-flow deposits, although the evidence for low and high-density-turbidity-current deposition varies in these areas. The number of turbidite beds in Area I is higher than in all other areas, turbulent-flow-prone hybrid event beds are common in Areas II and III, most hybrid event beds have a lowermost H1-division formed by low and high-density turbidity currents, and many H4-divisions only have plane-parallel lamination and ripple cross-lamination (Table 3). Moreover, Areas I and III predominantly exhibit flute marks at the base of beds, which are formed by turbulent and turbulence-enhanced transitional flows (Peakall et al. 2020). Despite the dominance of turbulent-flow signatures in Areas I–III, there is also evidence for a downflow increase in the proportion on transitional and laminar-flow phases, i.e. from an increasing percentage of beds with H2 and H3-divisions, respectively (Table 3). However, the proportion of H3-missing transitional-flow-prone hybrid event beds shows an opposite basinward trend, decreasing from 84% in Area I to 21% in Area III. The large thickness of hybrid event beds in Area III, and to a lesser degree in Area II (Fig. 8), suggests that these areas form a depocenter, possibly related to a decrease in slope gradient between Areas I and II. This would lead to flow deceleration and bulking and promote cohesive freezing of debris flows, thus explaining the relatively large thickness of the H3-divisions in hybrid event beds (Fig. 8). Alternatively, the presence of mudstone rafts in H3-divisions in Areas II and III, and their absence in Area I, may indicate flow bulking by local scouring and delamination of the seabed, followed by cohesive freezing of debris flows (Fonnesu et al. 2016).

The increasing importance of transitional flow inferred for Area I to III continues into Areas IV and V. Turbulent, transitional, and laminar-flow signatures are equally common in the hybrid event beds in Area IV, and transitional and laminar-flow signatures are more common than turbulent-flow signatures in Area V. Area V has a large proportion of transitional-flow-prone hybrid event beds mainly with a H3-division, the vast majority of these beds have H2 and H3-divisions, and sole marks mainly comprise skim, prod and groove marks, formed by upper-transitional plug flows and quasi-laminar and fully laminar plug flows (Peakall et al. 2020). It is inferred that relatively dilute flows, including low-viscosity debris flows, were able to escape deposition in Areas II and III and continued as a mixture of turbulent, transitional and laminar flows to Area IV, and then as predominantly transitional and laminar flows to Area V. This progressive shift from turbulent to cohesive flow behavior, may have been caused by flow deceleration and increasing flow viscosity, following deposition of sand and silt, as proposed by Baker and Baas (2020). The maintenance of a gentle slope gradient after the inferred decrease in slope gradient between Areas I and II would have helped this process.

The dominance of transitional and laminar flows further increases from Area V to VII, but this trend is interrupted by a return to a larger proportion of turbulent-flow signatures, combined with frequent laminar-flow and common transitional-flow signatures, in Area VI (Table 3). This may indicate a local increase in slope gradient, thus temporarily causing the flows to accelerate and regain some of the turbulence lost in Area IV and V. It is unlikely that this resulted from a decrease in suspended clay concentration, because there is no evidence in the sedimentary successions that the flows lost significantly more cohesive clay in Area VI than in Area V. Turbulent-flow signatures are rare in Area VII. Instead, transitional-flow-prone hybrid event beds are numerous, mostly without a H3-division, but with common evidence for thick H5-divisions formed by mud-rich flows, as well as thin H2lr, H2bw, and H4bw/h subdivisions (cf. Baker and Baas 2020). Sole marks are rare in Area VII, but mainly comprise skim and groove marks, formed by upper-transitional plug flows and quasi-laminar and fully laminar debris flows (Peakall et al. 2020). When arriving in Area VII, the hybrid flows had deposited most of their sandy and silty suspended load, mud clasts had fully disintegrated, and the flows were probably thin, slow moving and rich in suspended clay and therefore turbulence-attenuated and strongly cohesive.

CONCLUSIONS

Detailed sedimentological observations in submarine lobe fringe and distal fringe deposits of the Aberystwyth Grits Group and Borth Mudstone Formation, Wales, U.K., reveal a large facies variability in complex beds, deposited under changing conditions from turbulent through transitional to laminar flow. Basinward, the deposits change from predominantly turbidites and turbulent-flow-prone hybrid event beds via a mixture of turbulent and transitional-flow-prone hybrid event beds to H3-missing hybrid event beds with transitional-flow and muddy-debrite signatures. Moreover, the observation, confirmed by embedded Markov-chain analysis, that turbulent-flow-prone hybrid event beds and transitional-flow-prone hybrid event beds with and without division H3 share common sedimentological properties and vertical-facies transitions with the hybrid-event-bed model of Haughton et al. (2009), except for the presence transitional-flow signatures, allowed for the integration of transitional-flow facies into this widely used hybrid-event-bed model. These transitional facies statistically occur most often between turbulent-flow and laminar-flow facies, which suggests more gradual flow transformations, involving progressively increasing flow cohesion, than in the Haughton et al. (2009) model. The field data also reveal three types of incomplete facies models: turbulent-flow-prone hybrid event beds, transitional-flow-prone hybrid event beds with division H3, and transitional-flow-prone hybrid event beds without division H3, where the turbulent-flow-prone hybrid event beds are the closest match to the Haughton et al. (2009) model. The Haughton et al. (2009) model could therefore be viewed as one component of a larger suite of hybrid event beds.

The extended hybrid-event-bed model is characterized by the following adaptations to the H1–H5 divisions:

- The presence of Bouma-type subdivisions in division H1, indicating deposition from high-density turbidity currents as well as tractional low-density turbidity currents.
- The presence of various transitional-flow signatures in division H2, such as large ripples, low-amplitude bed waves, and heterolithic sandstone–mudstone, alongside banded sandstone.
- Evidence for variable laminar-flow rheologies in division H3, ranging from mudstone rafts via smaller mud clasts to well-mixed silt and clay.
- The presence of both tractional sedimentary structures typical of Bouma-type turbidites covered by low-amplitude bed waves and sandstone-mudstone heterolithics formed by transitional flow in division H4.
- Evidence for laminar-mud-flow deposition, alongside hemipelagic deposition and slow deposition from the muddy tail of turbidity currents, in division H5.

Hybrid event beds can form under various conditions, controlled by allogenic and autogenic factors, for example through rapid flow transformation that leads to bypassing of flow types and lack of formation or preservation of certain facies, and through more gradual transformation, allowing for the preservation of a greater facies diversity and more complete hybrid event beds. The extended facies model for hybrid event beds shows that hybrid flows can have a complex structure in the late stage of flow, undergoing renewed turbulent–transitional–(quasi-)laminar flow evolution as a result of flow deceleration, preserved in the H4 and H5-divisions.

In light of the presented data, hybrid-flow deposits represent a much larger and more complex family of flows, whilst maintaining a coherent and predictable model of vertical-facies transitions. Therefore, their occurrence in other deep-water basins may be much more widespread than previously recognized. The extended hybrid-event-bed model presented here should find wide application beyond the research area, allowing for more accurate description of a wide spectrum of hybrid-flow deposits, and better understanding of depositional processes and locations of occurrence in various deep-water basins.

ACKNOWLEDGMENTS

The authors would like to thank the International Association of Sedimentologists (IAS) for funding PŁ's fieldwork in the Aberystwyth Grits Group and Borth Mudstone Formation. JHB's participation in the field work, subsequent data analysis and paper writing was partly funded by a grant from Equinor Norway. The authors express their thanks to Marco Patacci and the anonymous reviewer and to the editors Dustin Sweet and George Postma for their insightful and helpful comments that improved the quality of this work.

REFERENCES

Allen, J.R.L., 1982, Sedimentary Structures, Their Character and Physical Basis, v. 1, 2: Amsterdam, Elsevier, 593 p, 663 p.

Amy, L.A., AND Talling, P.J., 2006, Anatomy of turbidites and linked debrites based on long distance (120 × 30 km) bed correlation, Marnoso Arenacea Formation, Northern Apennines, Italy: Sedimentology, v. 53, p. 161–212.

Anketell, J.M., Cegła, J., AND Dżułyński, S., 1970, On the deformational structures in systems with reversed density gradients: Annales Societatis Geologorum Poloniae, v. 40, p. 3–30.

Arnott, R.W.C., AND Hand, B.M., 1989, Bedforms, primary structures and grain fabric in the presence of suspended sediment rain: Journal of Sedimentary Research, v. 59, p. 1062–1069.

Ashley, G.M., Southard, J.B., AND Boothroyd, J.C., 1982, Deposition of climbing-ripple beds: a flume simulation: Sedimentology, v. 29, p. 67–79.

Baas, J.H., AND Best, J.L., 2002, Turbulence modulation in clay-rich sediment-laden flows and some implications for sediment deposition: Journal of Sedimentary Research, v. 72, p. 336–340.

Baas, J.H., Best, J.L., Peakall, J., AND Wang, M., 2009, A phase diagram for turbulent, transitional, and laminar clay suspension flows: Journal of Sedimentary Research, v. 79, p. 162–183.

Baas, J.H., Best, J.L., AND Peakall, J., 2011, Depositional processes, bedform development and hybrid bed formation in rapidly decelerated cohesive (mud-sand) sediment flows: Sedimentology, v. 58, p. 1953–1987.

Baas, J.H., Best, J.L., AND Peakall, J., 2016, Predicting bedforms and primary current stratification in cohesive mixtures of mud and sand: Journal of the Geological Society, v. 173, p. 12–45.

Baas, J.H., Tracey, N.D., AND Peakall, J., 2021, Sole marks reveal deep-marine depositional process and environment: Implications for flow transformation and hybrid-event-bed models: Journal of Sedimentary Research, v. 91, p. 986–1009.

Baker, M.L., Baas, J.H., Malarkey, J., Silva Jacinto, R., Craig, M.J., Kane, I.A., AND Barker, S., 2017, The effect of clay type on the properties of cohesive sediment gravity flows and their deposits: Journal of Sedimentary Research, v. 87, p. 1176–1195.

Baker, M.L., AND Baas, J.H., 2020, Mixed sand–mud bedforms produced by transient turbulent flows in the fringe of submarine fans: indicators of flow transformation: Sedimentology, v. 67, p. 2645–2671.

Baker, M.L., AND Baas, J.H., 2023, Does sand promote or hinder the mobility of cohesive sediment gravity flows?: Sedimentology, v. 70, p. 1110–1130.

Barker, S.P., Haughton, P.D.W., McCaffrey, W.D., Archer, S.G., AND Hakes, B., 2008, Development of rheological heterogeneity in clay-rich high-density turbidity currents: Aptian Britannia Sandstone Member, U.K. Continental Shelf: Journal of Sedimentary Research, v. 78, p. 45–68.

Breien, H., De Blasio, F.V., Elverhøi, A., Nystruen, J.P., AND Harbitz, C.B., 2010, Transport mechanisms of sand in deep-marine environments – insights based on laboratory experiments: Journal of Sedimentary Research, v. 80, 975–990.

Bell, D., Stevenson, C.J., Kane, I.A., Hodgson, D.M., AND Poyatos-Moré, M., 2018, Topographic controls on the development of contemporaneous but contrasting basin-floor depositional architectures: Journal of Sedimentary Research, v. 88, p. 1166–1189.

Best, J.L., AND Bridge, J.S., 1992, The morphology and dynamics of low amplitude bedwaves upon upper stage plane beds and the preservation of planar laminae: Sedimentology, v. 39, p. 737–752.

Bouma, A., 1962, Sedimentology of Some Flysch Deposits: A Graphic Approach to Facies Interpretation: Amsterdam, Elsevier, 168 p.

Brooks, H.L., Ito, M., Zuchuat, V., Peakall, J., AND Hodgson, D.M., 2022, Channel-lobe transition zone development in tectonically active settings: Implications for hybrid bed development: The Depositional Record, v. 8, p. 829–868.

Cherns, L., Cocks, L.R.M., Davies, J.R., Hillier, R.D., Waters, R.A., AND Williams, M., 2006, Silurian: the influence of extensional tectonics and sea-level changes on sedimentation in the Welsh Basin and on the Midland Platform, *in* Brenchley, P.J. and Rawson, P.F., eds., The Geology of England and Wales: The Geological Society, London, p. 75–102.

Davies, J.R., Fletcher, C.J.N., Waters, R.A., Woodhall, D.G., AND Zalasiewicz, J.A., 1997, Geology of the Country Around Llanilar and Rhayader: Stationary Office, London, British Geological Survey Memoir, Sheets 178 and 179 (England and Wales).

Davis, J.C., 2002, Statistics and Data Analysis in Geology (3rd ed.): John Wiley & Sons, New York, 638 p.

Davis, C.E., Haughton, P.D.W., McCaffrey, W.D., Scott, E., Hogg, N., AND Kitching, D., 2009, Character and distribution of hybrid sediment gravity flow deposits from the outer Forties Fan, Palaeocene Central North Sea, UKCS: Marine Petroleum Geology, v. 26, p. 1919–1939.

de Vet, M.G.W., Fernández, R., Baas, J.H., McCaffrey, W.D., AND Dorrell, R.M., 2023, Streamwise turbulence modulation in non-uniform open-channel clay suspension flows: Journal of Geophysical research, Earth Surface, v. 128, e2022JF006781.

Dodd, T.J., McCarthy, D.J., Amy, L., Plenderleith, G.E., AND Clarke, S.M., 2022, Hybrid event bed character and distribution in the context of ancient deep-lacustrine fan models: Sedimentology, v. 69, p. 1891–1926.

Fonnesu, M., Haughton, P., Felletti, F., AND McCaffrey, W., 2015, Short length-scale variability of hybrid event beds and its applied significance: Marine and Petroleum Geology, v. 67, p. 583–603.

Fonnesu, M., Patacci, M., Haughton, P.D.W., Felletti, F., AND McCaffrey, W.D., 2016, Hybrid event beds generated by local substrate delamination on a confined-basin floor: Journal of Sedimentary Research, v. 86, p. 929–943.

Fonnesu, M., Felletti, F., Haughton, P.D.W., Patacci, M., AND McCaffrey, W.D., 2018, Hybrid event bed character and distribution linked to turbidite system sub-environments: the North Appenine Gottero Sandstone (north-west Italy): Sedimentology, v. 65, p. 151–190.

Gladstone, C., McClelland, H.L.O., Woodcock, N.H., Pritchard, D., AND Hunt, J.E., 2018, The formation of convolute lamination in mud-rich turbidites: Sedimentology, v. 65, p. 1800–1825.

Grundvåg, S.-A., Johannessen, E.P., Helland-Hansen, W., AND Plink-Björklund, P., 2014, Depositional architecture and evolution of progradationally stacked lobe complexes in the Eocene Central Basin of Spitsbergen: Sedimentology, v. 61, p. 535–569.

Hansen, L.A.S., Hodgson, D.M., Pontén, A., Bell, D., AND Flint, S., 2019, Quantification of basin-floor fan pinchouts: examples from the Karoo Basin, South Africa: Frontiers in Earth Science, v. 7, doi:10.3389/feart.2019.00012.

Haughton, P.D.W, Barker, S.P., AND McCaffrey, W.D., 2003, ‘‘Linked’’ debrites in sand-rich turbidite systems: origin and significance: Sedimentology, v. 50, p. 459–482.

Haughton, P.D.W., Davis, C., McCaffrey, W., AND Barker, S.P., 2009, Hybrid sediment gravity flow deposits – classification, origin and significance, *in* Amy, L.A., McCaffrey, W.B., Talling, P.J., eds., Hybrid and Transitional Submarine Flows: Marine Petroleum Geology, v. 26, p. 1900–1918.

Hodgson, D.M., 2009, Distribution and origin of hybrid beds in sand-rich submarine fans of the Tanqua depocentre, Karoo Basin, South Africa: Marine Petroleum Geology, v. 26, p. 1940–1956.

Hussain, A., Haughton, P.D.W., Shannon, P.M., Turner, J.N., Pierce, C.S., Obradorslatre, A., Barker, S.P., AND Martinsen, O.J., 2020, High-resolution X-ray fluorescence profiling of hybrid event beds: implications for sediment gravity flow behaviour and deposit structure: Sedimentology, v. 67, p. 2850–2882.

Ilstad, T., Marr, J.G., Elverhøi, A., AND Harbitz, C.B., 2004, Laboratory studies of subaqueous debris flows by measurements of pore-fluid pressure and total stress: Marine Geology, v. 213, 403–414.

Iverson, R.M., 1997, Physics of debris flows: Reviews of Geophysics, v. 35, p. 245–296.

Jopling, A.V., AND Walker, R.G., 1968, Morphology and origin of ripple-drift cross-lamination, with examples from the Pleistocene of Massachusetts: Journal of Sedimentary Research, v. 38, p. 971–984.

Kane, I.A., AND Pontén, A.S.M., 2012, Submarine transitional flow deposits in the Paleogene Gulf of Mexico: Geology, v. 40, p. 1119–1122.

Kane, I.A., Pontén, A.S.M., Vangdal, B., Eggenhuisen, J.T., Hodgson, D.M., AND Spychala, Y.T., 2017, The stratigraphic record and processes of turbidity current transformation across deep-marine lobes: Sedimentology, v. 64, p. 1236–1273.

Kneller, B., 1995, Beyond the turbidite paradigm: physical models for deposition of turbidites and their implications for reservoir prediction, *in* Hartley, A.J. and Prosser, D.J, eds., Characterisation of Deep Marine Clastic Systems: Geological Society of London, Special Publication, v. 94, p. 29–46.

Kneller, B.C., AND Brannery, M.J., 1995, Sustained high-density turbidity currents and the deposition of thick massive sands: Sedimentology, v. 42, p. 607–616.

Kneller, B., AND Buckee, C., 2000, The structure and fluid mechanics of turbidity currents: a review of some recent studies and their geological implications: Sedimentology, v. 47, p. 62–94.

Kuswandaru, G.Y., Amir Hassan, M.H., Matenco, L.C., Taib, N.I., AND Mustapha, K.A., 2018, Turbidite, debrite, and hybrid event beds in submarine lobe deposits of the Palaeocene to middle Eocene Kapit and Pelagus members, Belaga Formation, Sarawak, Malaysia: Geological Journal, v. 54, p. 3421–3437.

Lowe, D.R., 1982, Sediment gravity flows, II. Depositional models with special reference to the deposits of high-density turbidity currents: Journal of Sedimentary Petrology, v. 52, p. 279–297.

Lowe, D.R., AND Guy, M., 2000, Slurry-flow deposits in the Britannia Formation (Lower Cretaceous), North Sea: a new perspective on the turbidity current and debris flow problem: Sedimentology, v. 47, p. 31–70.

Lowe, D.R., Guy, M., AND Palfrey, A., 2003, Facies of slurry-flow deposits, Britannia Formation (Lower Cretaceous), North Sea: implications for flow evolution and deposit geometry: Sedimentology, v. 50, p. 45–80.

Łapcik, P., 2023, Transitional flow deposits on submarine lobe flank (Veřovice and Lhoty Fms, Albian – Cenomanian, Polish Outer Carpathians): Sedimentary Geology, v. 445, 106329.

McClelland, H.L.O., Woodcock, N.H., AND Gladstone, C., 2011, Eye and sheath folds in turbidite convolute lamination: Aberystwyth Grits Group, Wales: Journal of Structural Geology, v. 33, p. 1140–1147.

Mueller, P., Patacci, M., AND Di Giulio, A., 2021, Hybrid event distribution in a mixed siliciclastic–calcareous turbidite succession: a cross-current perspective from the Bordighera Sandstone, Ligurian Alps, NW Italy: Italian Journal of Geosciences, v. 140, p. 255–274.

Mulder, T., 2011, Gravity processes and deposits on continental slope, rise and abyssal plains. *in* Hüeneke, H. and Mulder, T., eds., Deep-Sea Sediments: Developments in Sedimentology, Elsevier, Amsterdam, v. 63, p. 25–148.

Mulder, T., AND Alexander, J., 2001, The physical character of subaqueous sedimentary density flows and their deposits: Sedimentology, v. 48, p. 269–299.

Muzzi Magalhaes, P., AND Tinterri, R., 2010, Stratigraphy and depositional setting of slurry and contained (reflected) beds in the Marnoso-arenacea Formation (Langhian-Serravallian) Northern Apennines, Italy: Sedimentology, v. 57, p. 1685–1720.

Obradors-Latre, A., Haughton, P.D., Pierce, C.S., Shannon, P.M., Lacchia, A.R., Barker, S.P., AND Martinsen, O.J., 2023, Flow transformations, Mud Partitioning, and the Variable Stratigraphic Architecture of Basin-Floor Fan Fringes. Journal of Sedimentary Research, v. 93, p. 656–692.

Patacci, M., Haughton, P.D., AND McCaffrey, W.D., 2014, Rheological complexity in sediment gravity flows forced to decelerate against a confining slope, Braux, SE France: Journal of Sedimentary Research, v. 84, p. 270–277.

Peakall, J., Best, J., Baas, J.H., Hodgson, D.M., Clare, M.A., Talling, P.J., Dorrell, R.M., AND Lee, D.R., 2020, An integrated process-based model of flutes and tool marks in deep-water environments: implications for palaeohydraulics, the Bouma sequence and hybrid event beds: Sedimentology, v. 67, p. 1601–1666.

Pickering, K.T., AND Hiscott, R.N., 2015, Deep Marine Systems: Processes, Deposits, Environments, Tectonics and Sedimentation: John Wiley & Sons, London, 672 p.

Pierce, C.S., Haughton, P.D.W., Shannon, P.M., Pulham, A.J., Barker, S.P., AND Martinsen, O.J., 2018, Variable character and diverse origin of hybrid event beds in a sandy submarine fan system, Pennsylvanian Ross Sandstone Formation, western Ireland: Sedimentology, v. 65, p. 952–992.

Piper, D.J.W., Stow, D.A.V., AND Normark, W.R., 1984, The Laurentian Fan: Sohm Abyssal Plain: Geo-Marine Letters, v. 3, p. 141–146.

Pszonka, J., Wendorff, M., AND Godlewski, P., 2023, Sensitivity of marginal basins in recording global icehouse and regional tectonic controls on sedimentation. Example of the Cergowa Basin,(Oligocene) Outer Carpathians: Sedimentary Geology, v. 444, 106326.

Shanmugam, G., AND Moiola, R.J., 1995, Reinterpretation of depositional processes in a classic flysch sequence (Pennsylvanian Jackfork Group), Ouachita Mountains, Arkansas and Oklahoma: AAPG Bulletin, v. 79, p. 672–695.

Siwek, P., Waśkowska, A., AND Wendorff, M., 2023, Mud-rich low-density turbidites in structurally-controlled intraslope mini-basin: the influence of flow containment on depositional processes and sedimentation patterns (Szczawa, Oligocene, Polish Outer Carpathians): Sedimentology, v. 70, p. 1741–1784.

Smith, R., 2004, Turbidite systems influenced by structurally induced topography in the multi-sourced Welsh Basin. *in* Lomas, S.A., ed., Confined Turbidite Systems: Geological Society of London, Special Publication, v. 222, p. 209–228.

Southern, S.J., Kane, I.A., Warchoł, M.J., Porten, K.W., AND McCaffrey, W.D., 2017, Hybrid event beds dominated by transitional-flow facies: character, distribution and significance in the Maastrichtian Springar Formation, north-west Vøring Basin, Norwegian Sea: Sedimentology, v. 64, p. 747–776.

Spychala, Y.T., Hodgson, D.M., AND Lee, D.R., 2017, Autogenic controls on hybrid bed distribution in submarine lobe complexes: Marine and Petroleum Geology, v. 88, p. 1078–1093.

Stevenson, C.J., Talling, P.J., Masson, D.G., Sumner, E.J., Frenz, M., AND Wynn, R.B., 2014, The spatial and temporal distribution of grain-size breaks in turbidites: Sedimentology, v. 61, p. 1120–1156.

Stevenson, C.J., Peakall, J., Hodgson, D.M., Bell, D., AND Privat, A., 2020, T_B or not T_B: Banding in turbidite sandstones: Journal of Sedimentary Research, v. 90, p. 821–842.

Stow, D.A., AND Shanmugam, G., 1980, Sequence of structures in fine-grained turbidites: comparison of recent deep-sea and ancient flysch sediments: Sedimentary Geology, v. 25, p. 23–42.

Stow, D., AND Smillie, Z., 2020, Distinguishing between deep-water sediment facies: Turbidites, contourites and hemipelagites: Geosciences, v. 2, 43 p.

Talling, P.J., 2013, Hybrid submarine flows comprising turbidity current and cohesive debris flow: deposits, theoretical and experimental analyses, and generalized models: Geosphere, v. 9, p. 460–488.

Talling, P.J., Amy, L.A., Wynn, R.B., Peakall, J., Robinson, M., 2004, Beds comprising debrite sandwiched within co-genetic turbidite: origin and widespread occurrence in distal depositional environments: Sedimentology, v. 51, p. 163–194.

Talling, P.J., Masson, D.G., Sumner, E.J., AND Malgesini, G., 2012, Subaqueous sediment density flows: depositional processes and deposit types: Sedimentology, v. 59, p. 1937–2003.

Talling, P.J., Wynn, R.B., Masson, D.G., Frenz, M., Cronin, B.T., Schiebel, R., Akhmetzhanov, A.M., Dallmeier Tiessen, S., Benetti, S., Weaver, P.P.E., Georgiopoulou, A., Zuhlsdorff, C., AND Amy, L.A., 2007, Onset of submarine debris flow deposition far from original giant landslide: Nature, v. 450, p. 541–544.

Terlaky, V., AND Arnott, R.W.C., 2014, Matrix-rich and associated matrix-poor sandstones: avulsion splays in slope and basin-floor strata: Sedimentology, v. 61, p. 1175–1197.

Tinterri, R., AND Muzzi Magalhaes, P., 2011, Synsedimentary structural control on foredeep turbidites: an example from Miocene Marnoso-arenacea Formation, Northern Apennines, Italy: Marine and Petroleum Geology, v. 28, p. 629–657.

Tucker, M.E., 1982, The Field Description of Sedimentary Rocks: Geological Society of London Handbook, Open University Press, Milton Keynes, UK & John Wiley & Sons, New York. 112 p.

Wang, Y., Wignall, P.B., Peakall, J., Baas, J.H., AND Poulton, S.W., 2024, Soft-grounds: substrates controlled by sediment gravity flows and the evolution of deep-water trace fossils: Sedimentology, in review.

Wilson, D., Davies, J., Walters, R., AND Zalasiewicz, J., 1992, A fault-controlled depositional model for the Aberystwyth Grits turbidite system: Geological Magazine, v. 129, p. 595–607.

Wood, A., AND Smith, A.J., 1958, The sedimentation and sedimentary history of the Aberystwyth Grits (Upper Llandoverian): Quarterly Journal of the Geological Society, v. 114, p. 163–195.

FIGURE AND TABLE CAPTIONS

Table 1.—Description of sedimentary facies in the study area.

Table 2.—Overview of facies and subfacies codes used to describe the internal organization of hybrid event beds in the study area.

Table 3.—Summary of evidence for turbulent, transitional and laminar-flow signatures in the hybrid event beds of Areas I to VII.

Fig. 1. — Log of idealized hybrid event bed with inferred processes of formation of H1 to H5 divisions, based on Haughton et al. (2009).

Fig. 2.—Location maps of the study area. **A)** Geological map of the Aberystwyth Grits Group (comprising Mynydd Bach and Trefechan Formations) and Borth Mudstone Formation in Wales. Modified after Davies et al. (1997) and McClelland et al. (2011). **B)** Map of study area between Borth and Aberystwyth subdivided into seven smaller areas (I–VII).

Fig. 3.—Variety of appearances of and upward-changing structures in hybrid event beds. **A)** Bipartite H3-division with lower muddy sandstone bearing rare scattered small mud clasts and sandy ball-and-pillow structures, and upper part with high concentration of large, elongated mud clasts aligned

parallel to the bed surface. Area IV. **B)** Hybrid event bed with graded sandstone (H1m) capped by banded sandstone with load structures (H2b), muddy sandstone with scattered sandy ball-and-pillow structures (H3), heterolithic sandstone–mudstone (H4h) and massive black mudstone (H5). Area II. **C)** Lower part of hybrid event bed showing ripple-cross-laminated sandstone (H1r) with uneven, wavy top. Heterolithic sandstone–mudstone infills current-ripple troughs and partially drapes ripple surfaces (H2h). Area IV. **D, E, F)** Hybrid event beds showing a variety of Bouma-like sequences in division H1, including massive sandstone (H1m), plane-parallel-laminated sandstone (H1p) and cross-laminated sandstone (H1r). Area VI. **G)** Bipartite H3-division with muddy sandstone with scattered sandstone balls and pillows, overlain by sandy mudstone with plastically deformed streaks of siltstone (Area VI). Note variety of structures in subdivision H4 in pictures **A–C** and **G**. H1–H5 = hybrid-event-bed divisions. m = massive sandstone; p = plane-parallel lamination; r = ripple cross-lamination; b = banded sandstone; lr = large-ripple cross-lamination; bw = low-amplitude bed waves; h = heterolithic sandstone–mudstone.

Fig. 4.—Field examples of hybrid event beds. **A–C, E)** Examples of transitions of different H1-subdivisions, via different H2-subdivisions to division H3. Note division H3 in (E) is bipartite with chaotic muddy sandstone at the base and sandy mudstone at the top. (A) and (C) are from area VI, (B) is from area IV, and (E) is from area VII. **D)** Hybrid event bed with thin massive-sandstone division (H1m) passing into thick debritic division (H3), with plane-parallel-laminated sandstone (H4) disturbed by loading. Area II. **F)** Hybrid event bed that lacks division H1 and shows large ripples (H2lr) at its base instead (Area VI). H1–H5 = hybrid-event-bed divisions. m = massive sandstone; p = plane-parallel lamination; b = banded sandstone; lr = large-ripple cross-lamination; h = heterolithic sandstone–mudstone.

Fig. 5.—Field examples of transitional-flow deposits (Facies Association 5) . **A, C, E, F)** Transitional-flow deposits missing ‘classic’ Bouma-type divisions. **B, C, D)** Transitional-flow beds with ‘classic’ Bouma-type divisions at their base. Each picture is from area IV. H1–H5 = hybrid-event-bed divisions. m =

massive sandstone; p = plane-parallel lamination; r = ripple cross-lamination; b = banded sandstone; lr = large-ripple cross-lamination; bw = low-amplitude bed waves; h = heterolithic sandstone–mudstone; si = siltstone.

Fig. 6.—Results of embedded Markov-chain analysis plotted onto the original hybrid-event-bed model of Haughton et al. (2009) and presented as a flow-evolution tree on the basis of difference matrices for hybrid event beds in **A** (number of subdivision transitions = 450; confidence level of difference matrix = 99%)**,** transitional-flow deposits in **B** (number of subdivision transitions = 248; confidence level of difference matrix = 99%), and for combined hybrid event beds and transitional-flow deposits in **C** (number of subdivision transitions = 698; confidence level of difference matrix = 99%). H1–H5 = hybrid-event-bed divisions; m = massive sandstone; p = plane-parallel lamination; r = ripple cross-lamination; b = banded sandstone; lr = large-ripple cross-lamination; bw = low-amplitude bed waves; h = heterolithic sandstone–mudstone; d = debritic division; mm = massive mudstone.

Fig. 7.—Extended hybrid-event-bed model that combines the original turbulent-flow-prone model of Haughton et al. (2009) with beds that show a wider range of textures and sedimentary structures, and inferred flow types, based on observations in the Aberystwyth Grits Group and Borth Mudstone Formation between Aberystwyth and Borth. H1–H5 = hybrid-event-bed divisions; m = massive sandstone; p = plane-parallel lamination; r = ripple cross-lamination; b = banded sandstone; lr = large-ripple cross-lamination; bw = low-amplitude bed waves; h = heterolithic sandstone–mudstone; mm = massive mudstone.

Fig. 8.—Mean thickness of hybrid event beds and their subdivisions (H1–H5) in Areas I–VII for **A)** all beds and **B)** beds with a H3-division only.

Fig. 9.—**A)** Spatial distribution of hybrid-event-bed types in Areas I to VII. HEB(turb) = turbulent-flow-prone hybrid event beds; HEB(tr+H3) = transitional-flow-prone hybrid event beds with a H3-division; HEB(tr-H3) = transitional-flow-prone hybrid event beds without a H3-division. **B)** Spatial distribution of

the lowermost subdivision of the hybrid event beds in Areas I–VII. **C)** Spatial distribution of the subdivision immediately above massive sandstone (H1m) in the hybrid event beds in Areas I–VII. **D)** Spatial distribution of mud-clast sizes. Numbers in pie charts refer to number of bed types and subdivisions. H1, H2, H3 = hybrid-event-bed divisions; m = massive sandstone; p = plane-parallel lamination; r = ripple cross-lamination; b = banded sandstone; lr = large-ripple cross-lamination; bw = low-amplitude bed waves; h = heterolithic sandstone–mudstone.

Figure_1

Click here to access/download;Figure;Fig. 1_Haughton.jpg

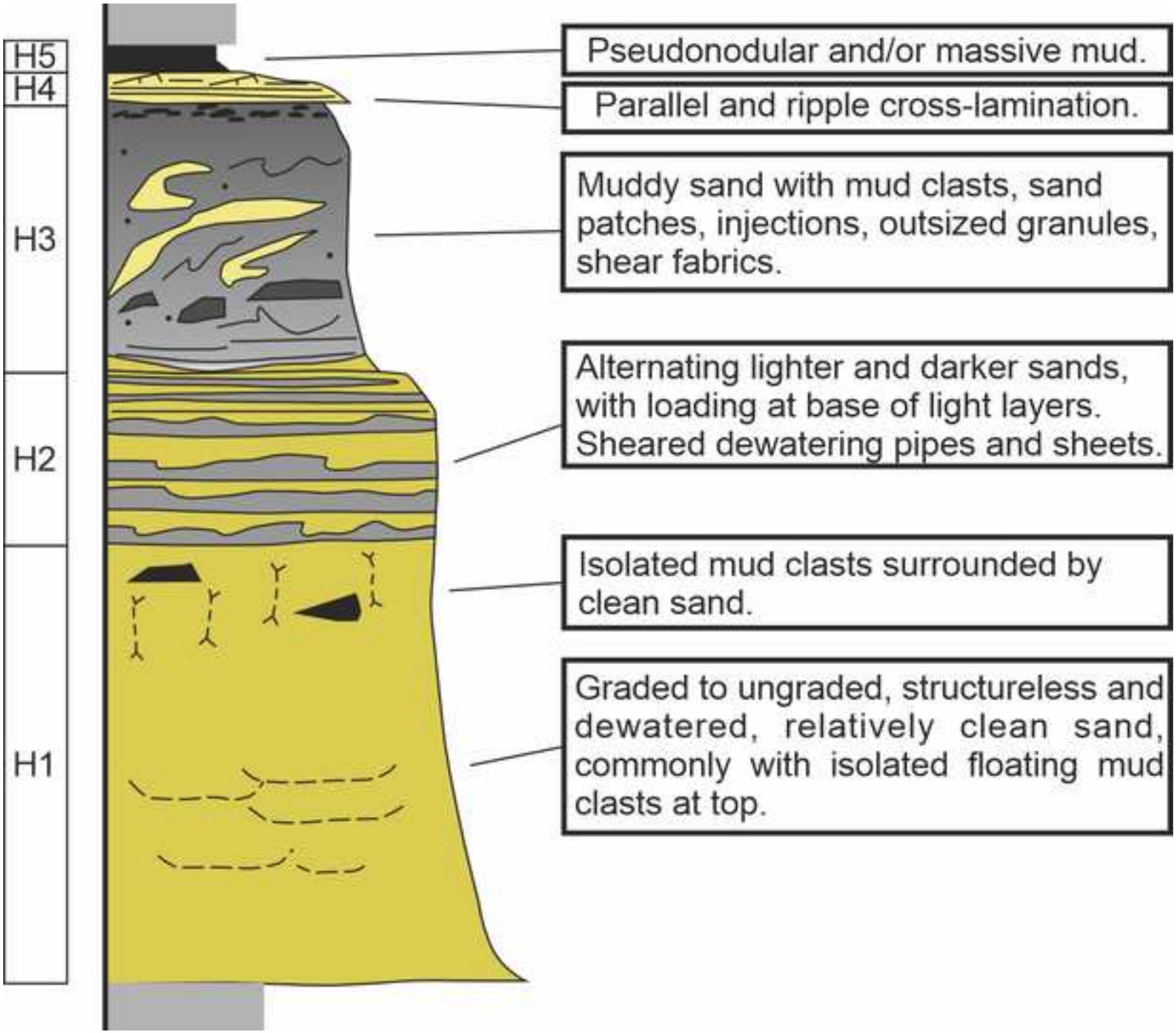

Figure_2

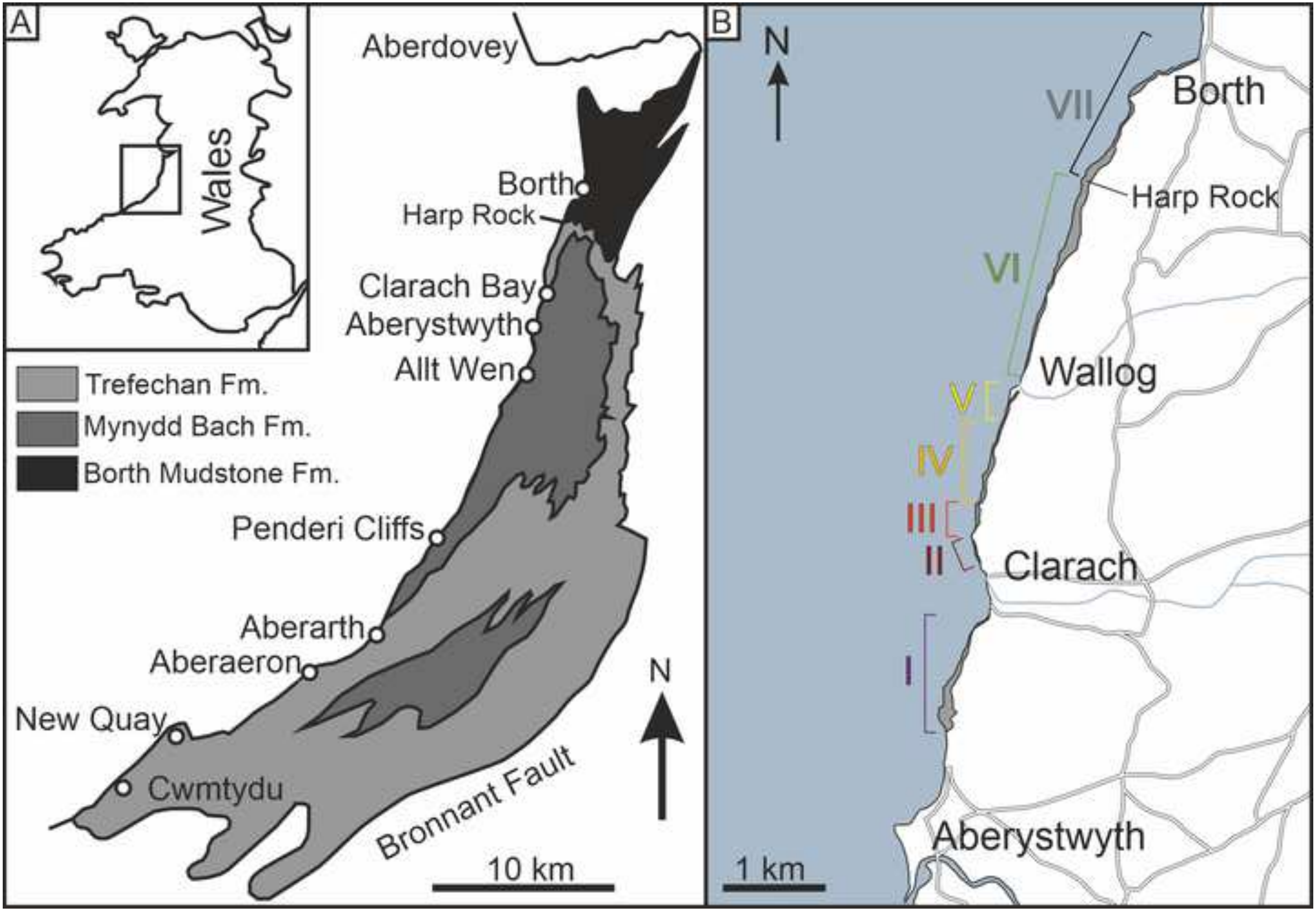
A
Wales
Aberdovey
Borth
Harp Rock
Clarach Bay
Aberystwyth
Allt Wen
Penderi Cliffs
Aberarth
Aberaeron
New Quay
Cwmtydu
Bronnant Fault
N
10 km
Trefechan Fm.
Mynydd Bach Fm.
Borth Mudstone Fm.
B
N
VII
Borth
Harp Rock
VI
Wallog
V
IV
III
II
Clarach
I
Aberystwyth
1 km

Figure_3

Click here to access/download;Figure;Fig. 3.jpg

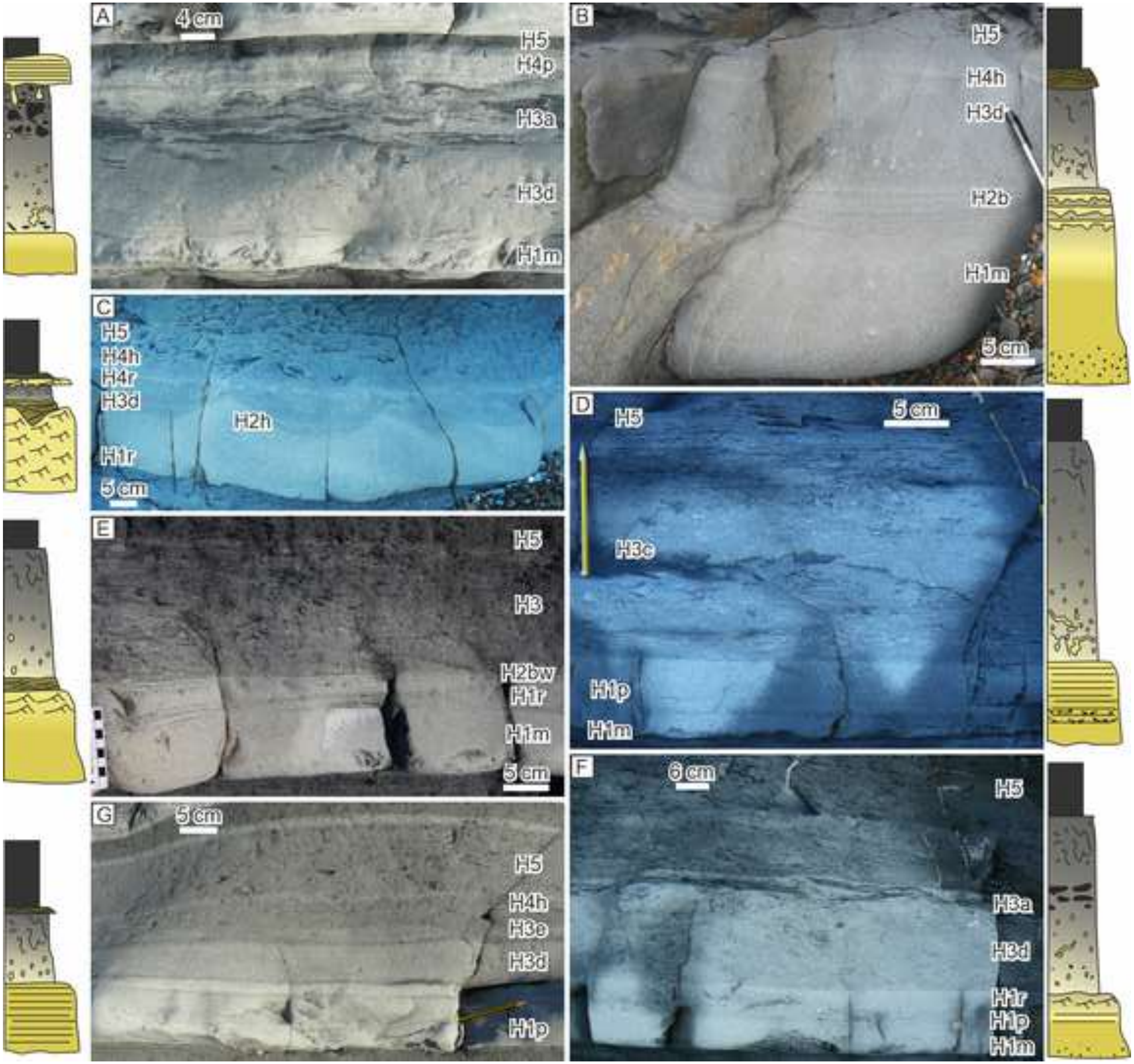

Figure_4

Click here to access/download;Figure;Fig. 4.jpg

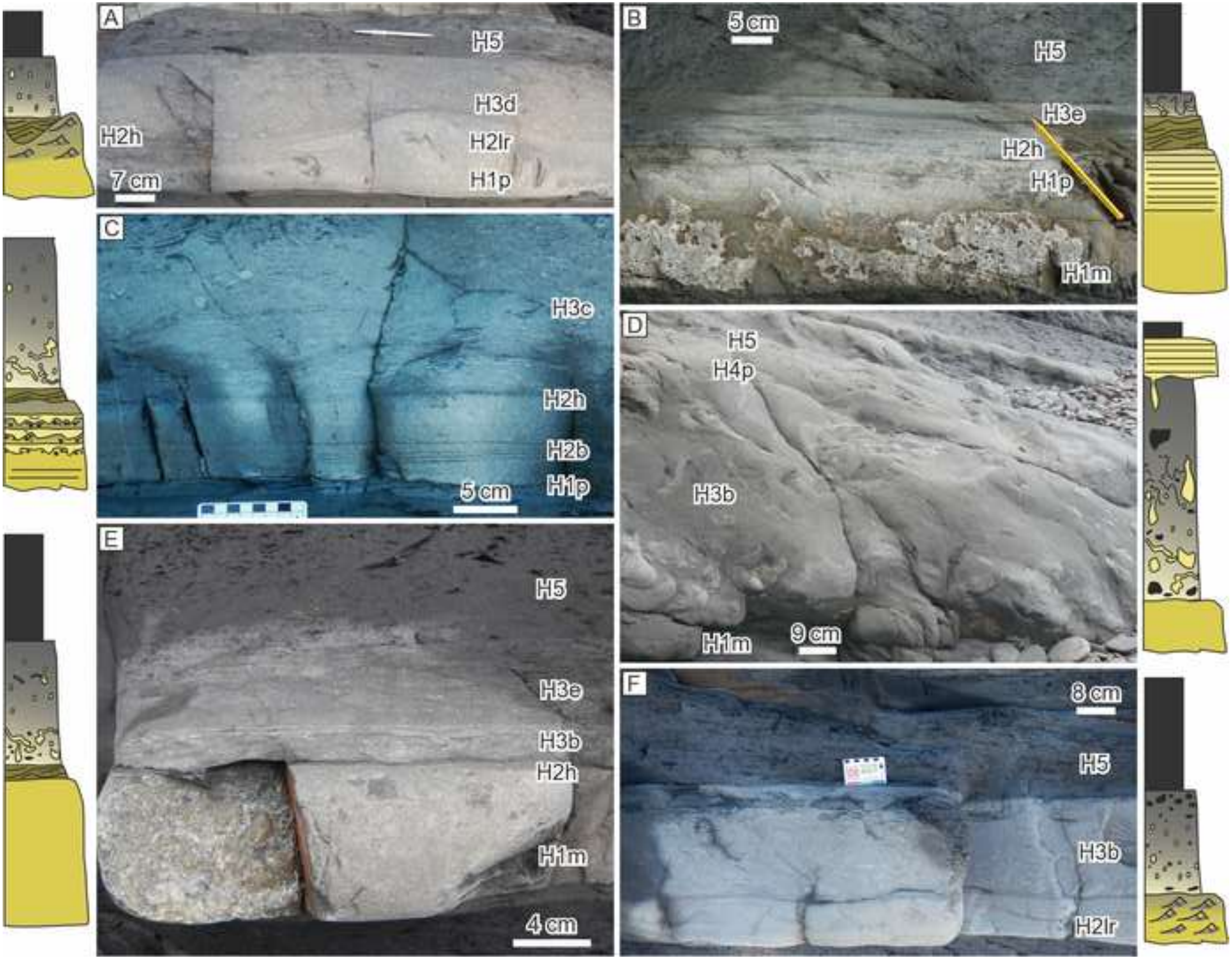

Figure_5

Click here to access/download;Figure;Fig. 5.jpg

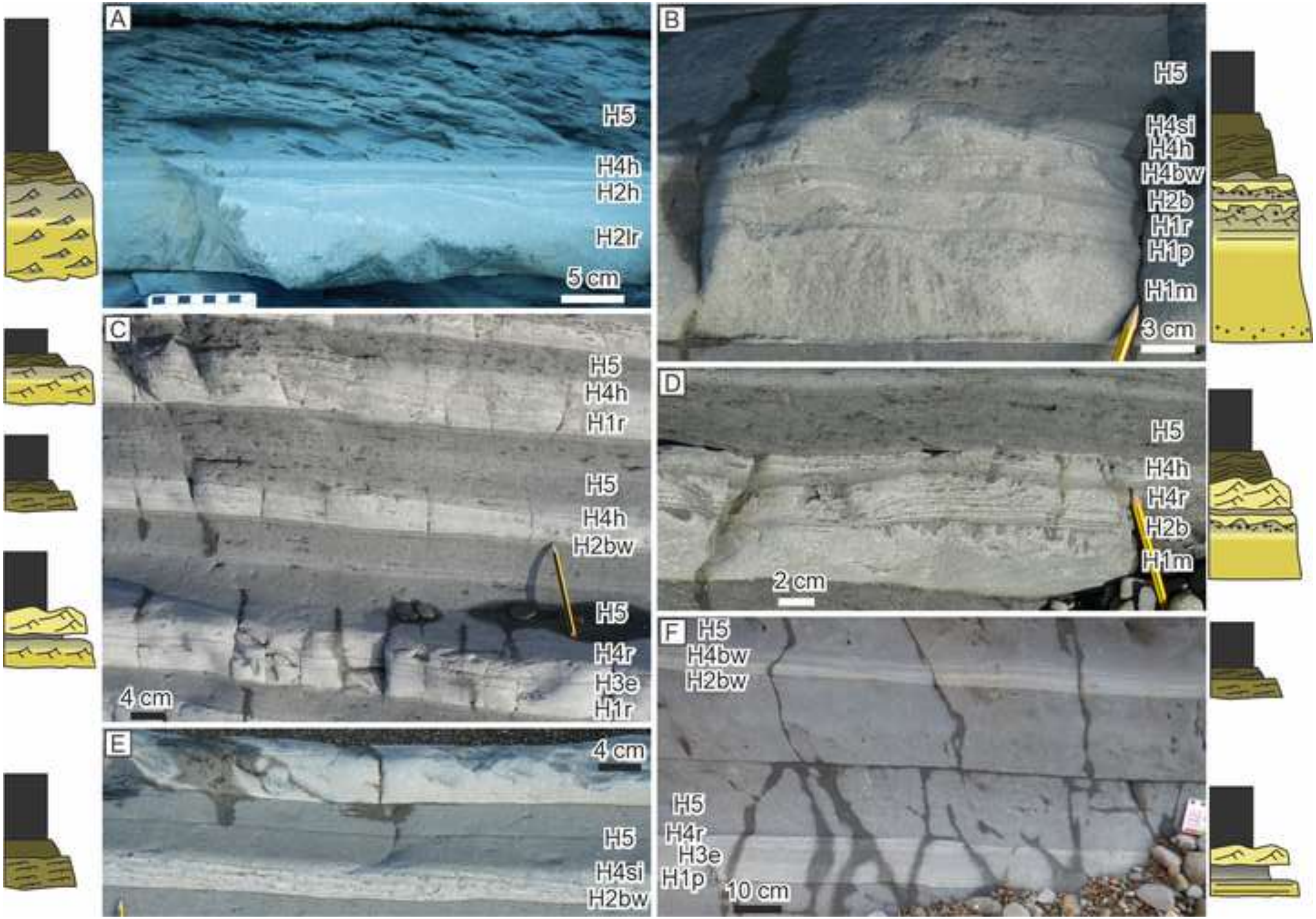

Figure_6

Click here to access/download;Figure;Fig. 6_Hybrid beds evolution map.jpg

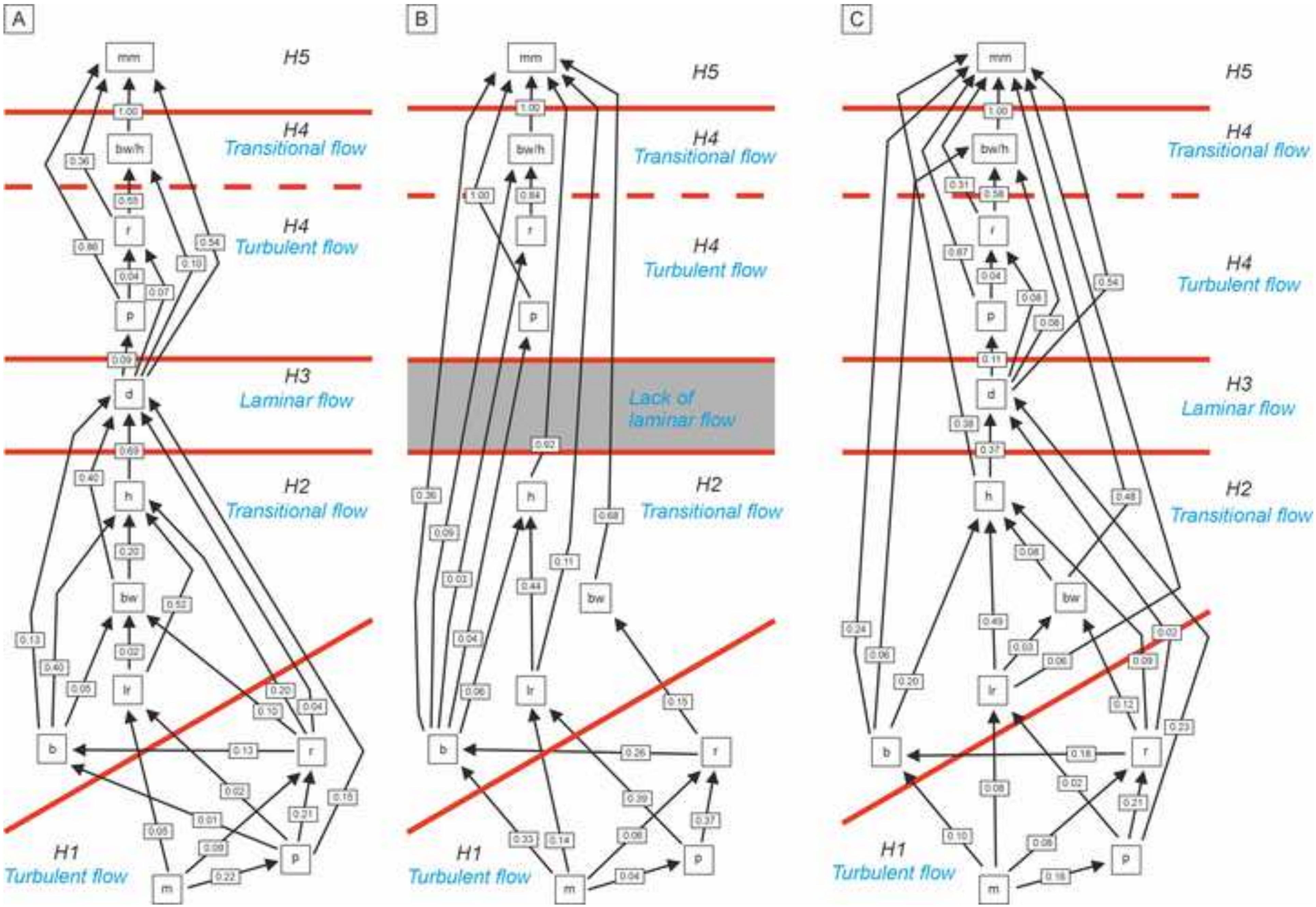

Figure_7

Click here to access/download;Figure;Fig. 7_New HEB model_noHaughton.jpg

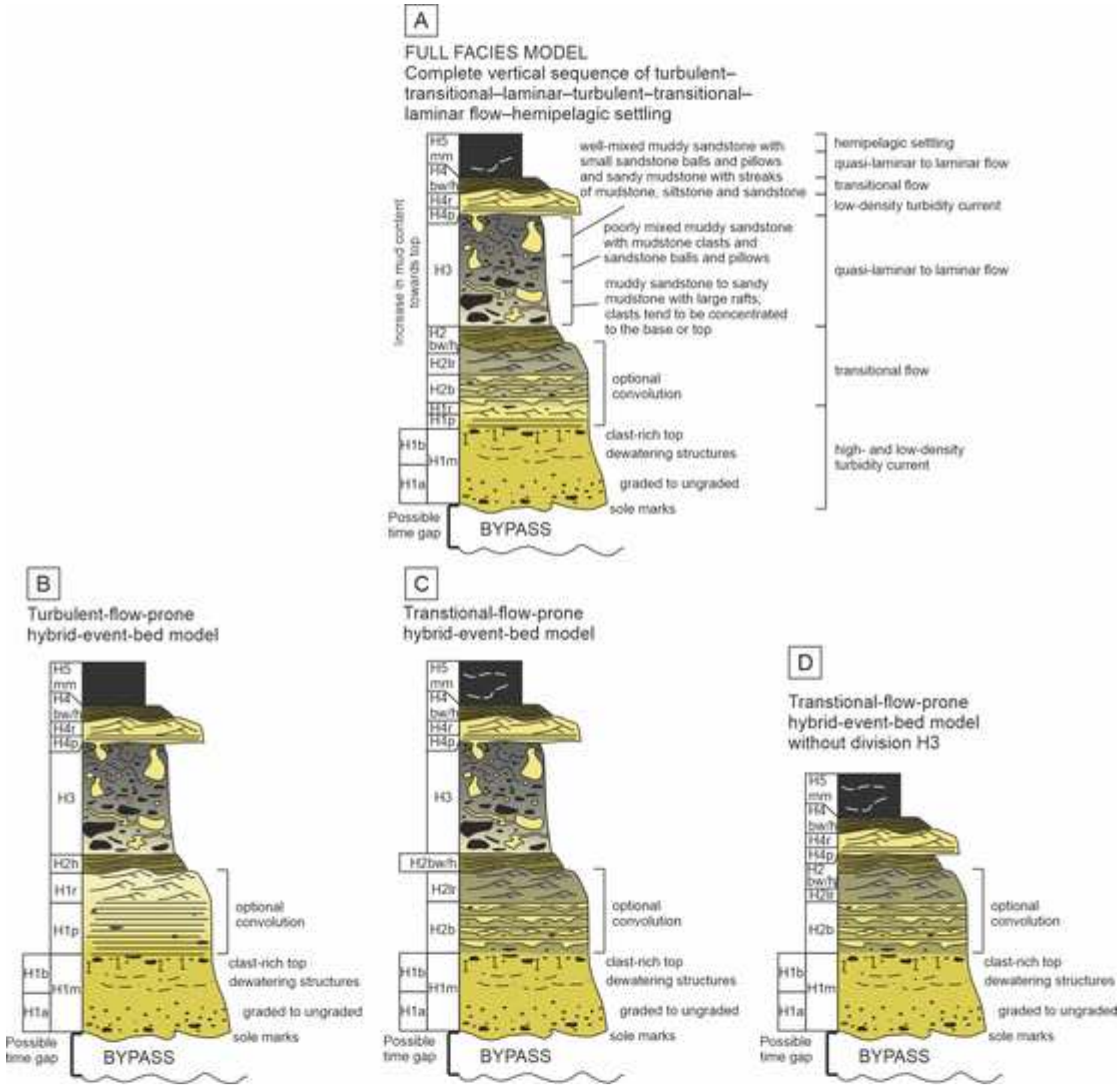

Figure_8

Click here to access/download;Figure;Fig. 8, bed thickness, distribution HEB.jpg

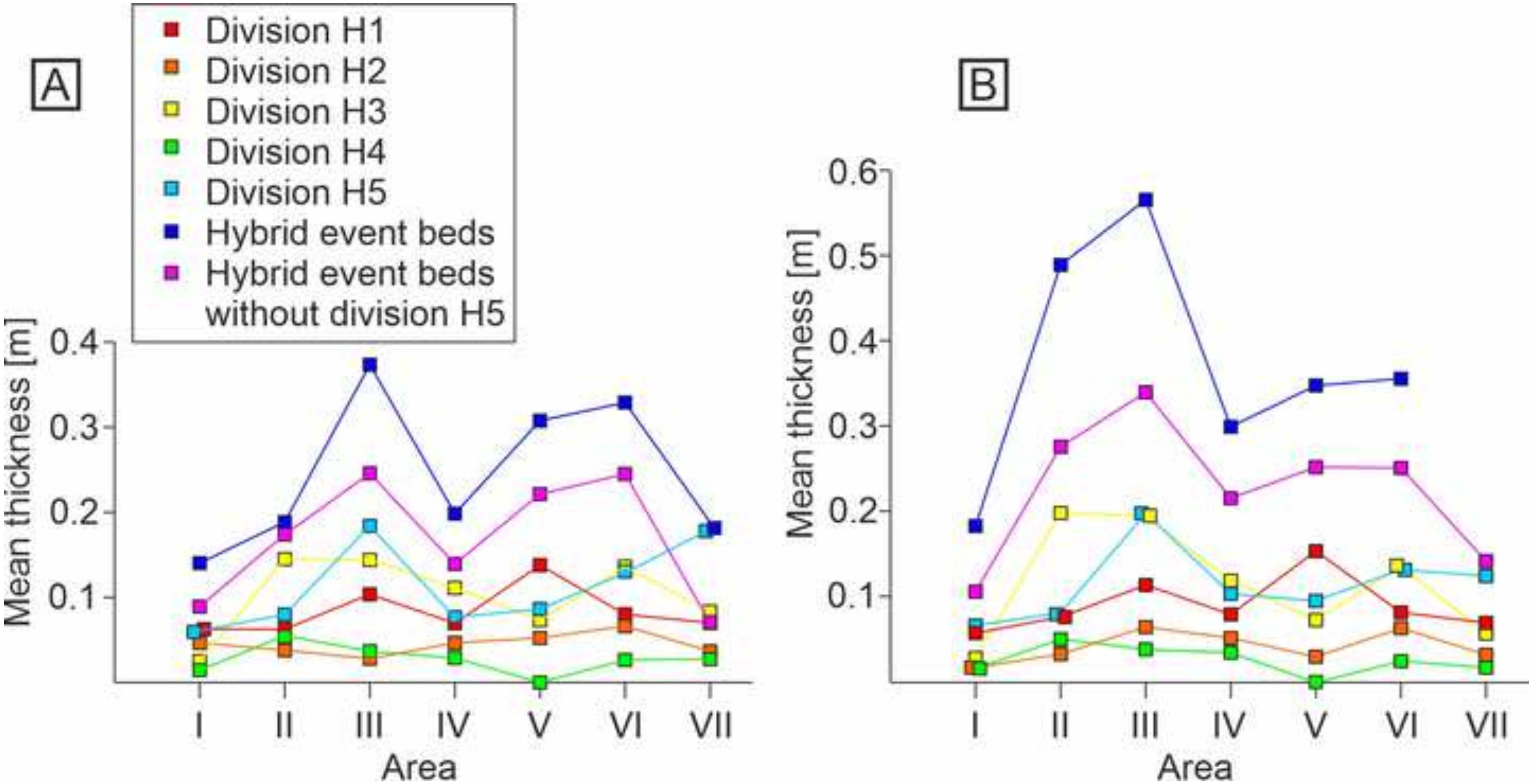

Figure_9

Click here to access/download;Figure;Fig. 9.jpg

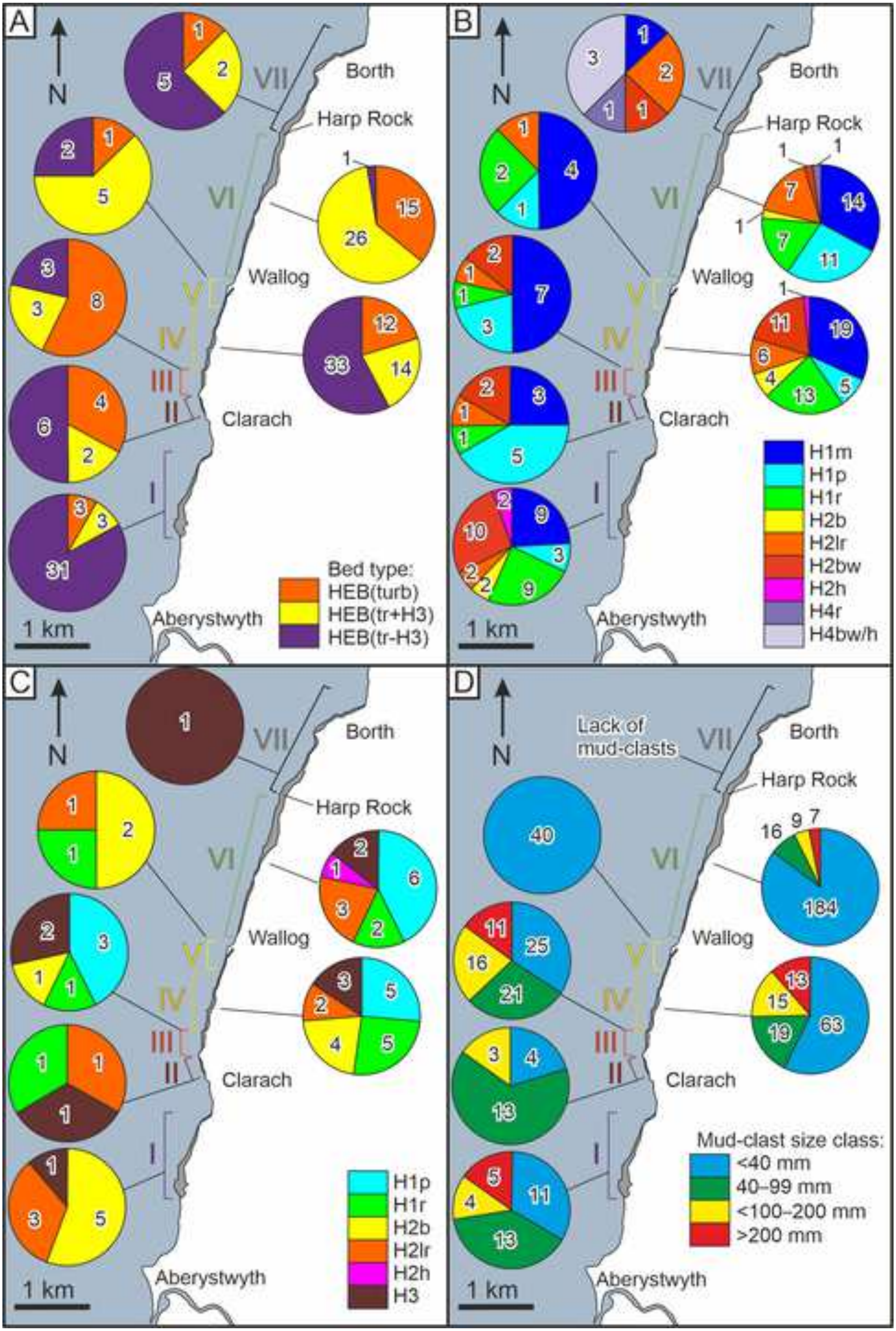

Table 1.— Description of sedimentary facies in the study area.

Sedimentary facies	**Main features**	**Process interpretation**
Massive sandstone 	Very-fine to medium-grained, structureless sandstone; graded to predominantly ungraded; sharp flat base; sharp top or gradually fining-upward; rarely wavy top	Rapid suspension fallout from sandy high-density turbidity current (Arnott and Hand 1989; Kneller and Branney 1995; Talling et al. 2012) or transient-turbulent flow (Baas et al. 2009, 2011)
Structured sandstone 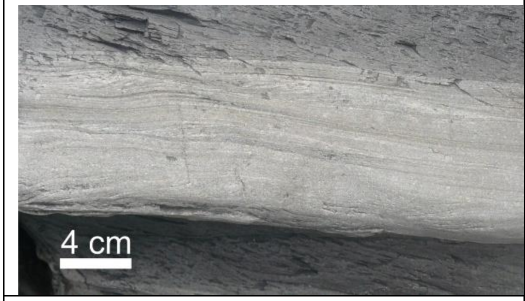	Very-fine to medium-grained, sandstone with plane-parallel lamination, wavy lamination, convolute lamination, ripple cross-lamination; sharp and predominantly flat base and top	Deposition from turbidity current; range of flow velocities, allowing generation of upper-stage plane bed and current ripples (Allen 1982; Best and Bridge 1992); soft sediment deformation forms wavy and convolute lamination
Banded sandstone 	Very-fine to fine-grained sandstone with distinctive dark and light bands; dark bands are rich in mud, light bands consist of massive sandstone; frequent soft-sediment deformation and loading of the light bands into dark bands	Transitional-flow deposits, reflecting pulsating turbulent and laminar flow (Lowe and Guy 2000; Lowe et al. 2003; Baas et al. 2009; Haughton et al. 2009; Stevenson et al. 2020; Łapcik 2023).
Clast-rich sandstone 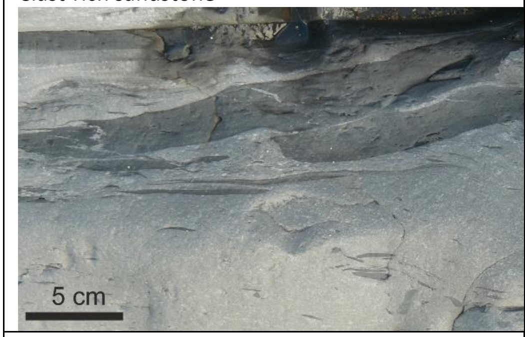	Very-fine to fine-grained, structureless, ungraded sandstone with dispersed mudstone, matrix-supported mudstone clasts and medium-grained sandstone clasts; clasts are well-rounded with preferred alignment parallel to the bedding; sharp, flat base and top	*En masse* freezing of cohesive, laminar debris flow or upper-transitional plug flow (Iverson 1997; Baas et al. 2009, 2011; Talling et al. 2012); well-rounded clasts suggest transformation from turbidity current
Structured muddy sandstone 	Mixture of very-fine to fine-grained sandstone, mixed sandstone–mudstone, siltstone and mudstone; large current ripples with angle of repose cross-lamination and low-amplitude bed-waves, often climbing	Rapidly decelerated turbulence-enhanced transitional flow (large ripples) and lower and upper transitional plug flow (low-amplitude bed waves) (Baas et al. 2016); simultaneous bedform migration and suspension fallout of mud

Heterolithic sandstone–mudstone 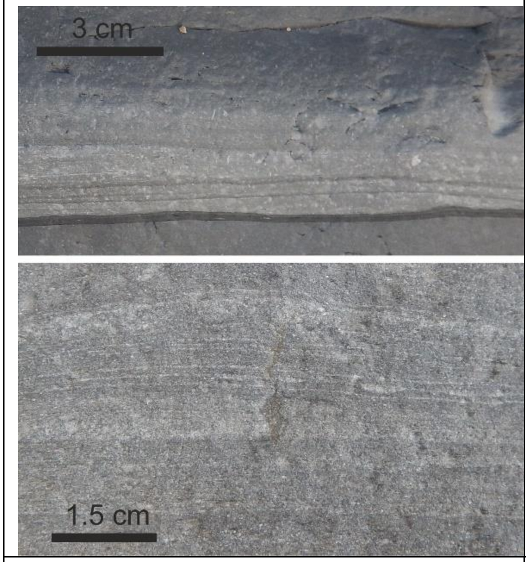	Alternation of laminae of fine-grained sandstone and mudstone with plane-parallel and wavy lamination; tendency to thickening of the mudstone laminae and thinning of sandstone laminae upward; flat, sharp or diffuse base, mostly flat and sharp top	i) Waxing and waning mixed sand–mud gravity flows (Kneller 1995); (ii) alternating deposition of sand from low-density turbidity current and suspension settling of mud; (iii) rapidly decelerated sand–mud transitional flow of constant velocity (Baas et al. 2016); (iv) simultaneous slow migration of sandy low-amplitude bed-waves (Best and Bridge 1992) and suspension fallout of mud (Baas et al. 2016); (v) slurry flows with near-bed shear sorting (Lowe and Guy 2000)
Siltstone 	Structureless to plane-parallel-laminated siltstone; normal grading with gradual top or ungraded with sharp top; flat boundaries and sharp base	Deposition from tractional turbidity current or lower-transitional plug flow (Piper et al. 1984; Baas et al. 2011; Talling et al. 2012)
Silty mudstone 	Structureless mudstone with dispersed silt particles; sharp base and top	Deposition from upper-transitional plug flows or quasi-laminar plug flow (Baas et al. 2011)
Mudstone 	Structureless mudstone; mostly flat and sharp base and top; occasional silty swirly textures	Hemipelagic settling or mud deposition from tail of sediment gravity flow (Bouma 1962; Talling et al. 2012); swirly textures form by *en masse* deposition from plug region of mud-rich, turbulence-attenuated flow (Baas et al. 2011; Stevenson et al. 2014)

Table 2.—Overview of facies and subfacies codes used to describe the internal organization of hybrid event beds in the study area.

Code	**Description**
H1m	Division H1 with massive sandstone
H1p	Division H1 with plane-parallel-laminated sandstone
H1r	Division H1 with ripple-cross-laminated sandstone
H2b	Division H2 with banded sandstone
H2lr	Division H2 with large ripples in structured muddy sandstone
H2bw	Division H2 with low-amplitude bed waves in structured muddy sandstone
H2h	Division H2 with heterolithic sandstone–mudstone
H3a	Division H3 with muddy sandstone large rafts consisting of mudstone or heterolithic mudstone–siltstone
H3b	Division H3 poorly mixed muddy sandstone with mudstone clasts and sandstone balls and pillows
H3c	Division H3 with muddy sandstone, lacking mudstone clasts, but with well-preserved sandstone pillows, present at all levels in the H3-division
H3d	Division H3 with well-mixed muddy sandstone with small sandstone clasts (pseudonodules), sandstone balls and pillows, and small mudstone clasts
H3e	Division H3 with sandy mudstone with streaks of mudstone, siltstone, and sandstone
H4p	Division H4 with plane-parallel-laminated sandstone
H4r	Division H4 with ripple-cross-laminated sandstone
H4bw/h	Division H4 with low-amplitude bed waves in structured muddy sandstone or heterolithic sandstone–mudstone
H4si	Division H4 composed of siltstone
H5mm	Division H5 composed of mudstone
HEB(turb)	Turbulent-flow-prone hybrid event bed
HEB(tr+H3)	Transitional-flow-prone hybrid event bed with a H3-division
HEB(tr-H3)	Transitional-flow-prone hybrid event bed without a H3-division

Table 3.—Summary of evidence for turbulent, transitional and laminar-flow signatures in the hybrid event beds of Areas I to VII.

Area	Evidence for turbulent flow	Evidence for transitional flow	Evidence for laminar flow	Flow interpretation
I	• Mainly turbidites throughout area • Most HEBs start with H1p or H1r • 70% of H4 in HEBs have only H4p/r • 75% of turbidites and HEBs have flute marks	• HEB(tr-H3) very common, but most lack H4 • Similar amounts of HEB(tr-H3) start with H1–H2 or H2-subdivision sequences • 92% of HEBs have H2 • 17% of beds have skim/prod marks	• 16% of HEBs have H3; mostly with swirly textures • 8% of beds have groove marks	Turbulent flows dominate (turbidites); HEBs mainly formed by transitional flows
II	• More HEB(turb) than in Area I • All HEB(turb) & HEB(tr+H3) start with H1 • 83% of H4 in HEBs have only H4p/r • 33% of beds have flute marks	• HEB(tr-H3) common, but less than in Area I • Equal amounts of HEB(tr-H3) start with H2 or H1 • 67% of HEBs have H2 • 50% of beds have skim/prod marks	• 50% of HEBs have H3; 17% with rafts • 17% of beds have groove marks	Turbulent flows dominate, mainly forming divisions below & above H3; more laminar flows than in Area I
III	• Mainly HEB(turb) • Most HEBs start with H1, forming Bouma-type sequences • 44% of H4 in HEBs have only H4p/r • 77% of beds have flute marks	• 43% of HEBs have H2 • 56% of H4 in HEBs have H4bw/h • 15% of beds have skim/prod marks	• 79% of HEBs have H3; 27% with rafts, 9% with swirly textures • 8% of beds have groove marks	Turbulent flows dominate, but also common laminar flows; transitional flows more common in later flow stages than in Areas I & II
IV	• HEB(turb) least common • Most HEBs start with H1, forming Bouma-type sequences • 56% of beds have flute marks	• HEB(tr-H3) common, starting with H1 or H2; some H1–H2-sequences • HEB(tr+H3) less common • 80% of HEBs have H2 (54% for HEB(turb) and HEB(tr+H3)) • 86% of H4 in HEBs have H4bw/h • 33% of beds have skim marks	• 44% of HEBs have H3, 18% with swirly textures • H3 become bi/tripartite (32%) • Some H1–H3-sequences • 11% of beds have groove marks	Turbulent, transitional & laminar flows all common
V	• No H4-divisions • Almost all HEBs start with H1 • 17% of beds have flute marks	• Mainly HEB(tr+H3); some HEB(tr-H3) • 87% of HEBs have H2, often in H1–H2–H3-sequences • 42% of beds have skim/prod marks	• 75% of HEBs have H3 • Well-mixed H3 with small mud clasts & pseudonodules • 42% of beds have groove marks	Transitional & laminar flows dominate, except for common turbulent flow in early stages
VI	• HEB(turb) less common • Most HEBs start with H1, forming Bouma-type sequences • 30% of H4 in HEBs have only H4p/r • 67% of beds have flute marks	• HEB(tr+H3) most common • Fewer HEBs start with H2 or have H1–H2-sequences • 70% of H4 in HEBs have H4bw/h • 20% of beds have skim marks	• 98% of HEBs have H3, 22% with swirly textures • 24% of H3 are bi/tripartite • 13% of beds have groove marks	Turbulent & laminar flows dominate; transitional flows also common, especially in later flow stages
VII	• HEB(turb) least common • One HEB starts with H1m, another with H2lr and H2bw • 25% of beds have flute marks	• HEB(tr-H3) common • HEB(tr+H3) less common • 75% of HEBs start with H2lr, H2bw, or H4bw/h • 38% of HEBs have H2 • All H4 in HEBs have H4bw/h • 50% of beds have skim marks	• Rare H3 with swirly textures, but very common H5 with swirly textures • 33% of H3 are bi/tripartite • 25% of beds have groove marks	Transitional & laminar flows dominate; only few turbulent flows

HEB(turb) = turbulent-flow-prone hybrid events beds; HEB(tr+H3) = transitional-flow-prone hybrid event beds with H3; HEB(tr-H3) = transitional-flow-prone hybrid event beds without H3. m = massive sandstone; p = plane-parallel lamination; r = ripple cross-lamination; lr = large ripple cross-lamination; bw = low-amplitude bed waves; h = heterolithic sandstone–mudstone.